



VCU

Virginia Commonwealth University
VCU Scholars Compass

Theses and Dissertations

Graduate School

2018

Targeting BCL-2 Family Members in the Cell Death Pathway to Treat Head and Neck Cancer

Erin L. Britt
Virginia Commonwealth University

Follow this and additional works at: <https://scholarscompass.vcu.edu/etd>

© The Author

Downloaded from

<https://scholarscompass.vcu.edu/etd/5352>

This Thesis is brought to you for free and open access by the Graduate School at VCU Scholars Compass. It has been accepted for inclusion in Theses and Dissertations by an authorized administrator of VCU Scholars Compass. For more information, please contact libcompass@vcu.edu.

© Erin Britt 2018
All Rights Reserved

TARGETING BCL-2 FAMILY MEMBERS IN THE CELL DEATH PATHWAY TO TREAT HEAD AND NECK CANCER

A thesis submitted in partial fulfillment of the requirements for the degree of Master of Science
at Virginia Commonwealth University

by

Erin L. Britt
George Washington University, B.S. 2016

Director: Hisashi Harada, Ph.D.
VCU School of Dentistry
Philips Institute for Oral Health Research

Virginia Commonwealth University
Richmond, VA
May 2018

Acknowledgement

I would like to thank many people who have supported me on this journey. First and foremost, I would like to sincerely express my gratitude toward my research advisor and primary investigator, Dr. Hisashi Harada. I cannot thank Dr. Harada enough for his continual support, guidance, and knowledge he has given me. His dedication to and passion for research has allowed me to enjoy my time working in his lab and develop a true appreciation for conducting experiments and analyzing their results.

I would also like to thank laboratory members Sung Woo Kim, Wade Cook, Yusrah Hasan, and Soo Lee, who have contributed greatly to my knowledge and made the work environment both positive and conducive to my project and enjoyment in the lab.

Additionally, I would like to express my gratitude to my committee members Dr. Qinglian Liu, Dr. Yue Sun, and Dr. Roland Pittman for their efforts and cooperation. I would also like to thank Dr. Yue Sun, Dr. Andrew Yeudall, and Dr. Iain Morgan for cell lines.

I am grateful to my family and friends who have supported and encouraged me throughout this project. Furthermore, I want to express my sincere gratitude to my parents who have remained a constant source of love, support, and inspiration, enabling me to pursue my dreams.

Table of Contents

List of Figures.....	v
List of Abbreviations.....	vii
Abstract.....	x
Chapter	
1 Introduction.....	1
1.1 Cancer.....	1
1.2 Head and Neck Cancer.....	2
1.3 Cell death.....	5
1.4 BCL-2 Family Members.....	8
1.5 Cisplatin.....	11
1.6 p53.....	14
1.7 NOXA and MCL-1.....	14
1.8 Fenretinide.....	18
1.9 ABT-263 (Navitoclax)	20
2 Hypothesis.....	23
3 Specific Aims.....	24
3.1 The first aim is to determine the underlying molecular mechanisms of cell death induced by Adenovirus-mediated NOXA expression (Ad-NOXA) or Ad-NOXA with ABT-263 combination treatment.....	24
3.2 The second aim is to determine the underlying molecular mechanisms of cell death induced by Fenretinide or Fenretinide with ABT-263 combination treatment.....	24

4 Materials and Methods.....	25
4.1 Cell lines and cell culture.....	25
4.2 Adenovirus production.....	25
4.3 Lentivirus production.....	26
4.4 Antibodies and Chemicals.....	26
4.5 Western blot analyses.....	27
4.6 Fluorescence Activated Cell Sorting (FACS) analyses.....	27
4.7 Crystal Violet Assay.....	28
4.8 Immunoprecipitation Analyses.....	28
4.9 Statistical Analyses.....	29
5 Results.....	30
5.1 Human HNSCC cell lines and characteristics.....	30
5.2 Ad-NOXA alone or Fenretinide alone can induce cell death in HN8.....	31
5.3 Ad-NOXA-induced cell death in HN8 is apoptosis.....	33
5.4 BAK contributes to NOXA-induced apoptosis.....	34
5.5 The mechanism of NOXA-induced cell death	35
5.6 Fenretinide alone can induce cell death in HN8.....	38
5.7 Ad-NOXA or Fenretinide combined with ABT-263 show synergistic effects in HN12.....	40
5.8 The role of BIM in Ad-NOXA and ABT-263 combination-induced cell death in HN12.....	42
5.9 Ad-NOXA or Fenretinide combined with ABT-263 shows increased cell death in other HNSCC cell lines.....	44

5.10 Mouse head and neck cancer cell lines and protein expression.....	47
5.11 Combinational treatment increases cell death in mouse HNSCC cells.	49
6 Discussion.....	54
6.1 NOXA-induced cell death leads to BAK activation.....	54
6.2 NOXA contributes to Fenretinide-induced cell death	55
6.3 Combinational treatment of ABT-263 with Ad-NOXA or Fenretinide enhanced cell death in HNSCC cells	56
6.4 Combinational treatment of ABT-263 with Ad-NOXA or Fenretinide was independent of p53 status.....	58
6.5 Mouse HNSCC cell lines are responsive to combinational treatment.....	59
7 Conclusion.....	60
Literature Cited.....	62
Vita.....	68

List of Figures

Figure 1: Locations of head and neck cancer.....	3
Figure 2: Apoptosis signaling pathways.....	7
Figure 3: BCL-2 family members as defined by BH domains.....	9
Figure 4: BCL-2 family members and function.....	10
Figure 5: BCL-2 family members mediate apoptosis in the mitochondrial pathway.....	11
Figure 6: Molecular structure of Cisplatin.....	12
Figure 7: Mechanism of action of Cisplatin.....	13
Figure 8: Sequences of human, rat and mouse NOXA.....	15

Figure 9: Mechanism of NOXA induction leads to apoptosis.....	17
Figure 10: Chemical structure of Fenretinide.....	19
Figure 11: Chemical structures of ABT-737 and ABT-263.....	21
Figure 12: Human HNSCC cell lines and characteristics.....	30
Figure 13: Ad-NOXA alone or Fenretinide alone can induce cell death in HN8.....	32
Figure 14: Ad-NOXA alone induces apoptosis in HN8.....	33
Figure 15: HN8 established shRNA knockdown cell lines for BAK (shBAK), BAX (shBAX), and BIM (shBIM)	34
Figure 16: BAK is contributing to cell death.....	35
Figure 17: HN8 Immunoprecipitation experiments show BCL-2 family member interactions....	37
Figure 18: The mechanism of cell death induced by NOXA.....	38
Figure 19: NOXA is contributing to Fenretinide-induced cell death	39
Figure 20: Ad-NOXA or Fenretinide in combination with ABT-263 has synergistic effects in HN12.	41
Figure 21: Combinational treatment of HN12 induces apoptosis.....	42
Figure 22: HN12 Immunoprecipitation with MCL-1 and HN12 BIM knockdown.....	43
Figure 23: HN12 BIM knockdown data.....	44
Figure 24: Ad-NOXA or Fenretinide in combination with ABT-263 increases cell death in UMSCC1.....	46
Figure 25: Ad-NOXA or Fenretinide in combination with ABT-263 has a synergistic effect in UMSCC47.....	47
Figure 26: Western Blot of mouse cell lines.....	48
Figure 27: Ad-NOXA and ABT-263 combinational treatment has a synergistic effect in 601,	

but Fenretinide and ABT-263 treatment does not produce as much cell death....	50
Figure 28: Ad-NOXA and Fenretinide in combination with ABT-263 increases cell death in 606.....	51
Figure 29: Ad-NOXA or Fenretinide with ABT-263 combinational treatment increases cell death in 602.....	52
Figure 30: Ad-NOXA and ABT-263 combinational treatment increases cell death in 613, but Fenretinide and ABT-263 treatment does not produce as much cell death.....	52
Figure 29: The mechanism of cell death induced by combinational treatment.....	61

Abbreviations

HNSCC: Head and neck squamous cell carcinoma

Rb: Retinoblastoma

DNA: Deoxyribonucleic acid

EGFR: Epidermal growth factor receptor

BCL-2: B-cell lymphoma 2

MCL-1: Myeloid cell leukemia 1

BCL-X_L: B-cell lymphoma-extra large

BAK: BCL-2 homologous antagonist killer

BAX: BCL-2 associated X protein

BAD: BCL-2 antagonist of cell death

BID: BH3 interacting domain

BIM: BCL-2 interacting mediator of cell death

PUMA: p53-upregulated modulator of apoptosis

HPV: Human papillomavirus

MOMP: Mitochondrial outer membrane permeabilization

APAF1: Apoptotic protease activating factor 1

TNF: Tumor necrosis factor

TNFR1: Tumor necrosis factor receptor 1

TNFR2: Tumor necrosis factor receptor 2

ER: Endoplasmic reticulum

BH: BCL-2 homology

OMM: Outer mitochondrial membrane

IMS: Intermembrane space

ATM: Ataxia telangiectasia mutated

ATR: ataxia telangiectasia and Rad3-related

MDM2: mouse double minute 2 homolog

E. coli: Escherichia coli

CDK2: cyclin dependent kinase 2

SCLC: Small cell lung cancer

Ad-NOXA: Adenovirus-mediated NOXA overexpression

PI: Propidium iodide

shRNA: Short hairpin RNA

cDNA: Complementary DNA

DMEM: Dulbecco's modified eagle medium

FBS: Fetal Bovine serum

PARP: Poly (ADP-Ribose) polymerase

4NQO: 4-nitroquinoline oxide

Ad-NOXA: Adenovirus-mediated NOXA overexpression

Ad-Con: Control adenovirus

Abstract

TARGETING BCL-2 FAMILY MEMBERS IN THE CELL DEATH PATHWAY TO TREAT HEAD AND NECK CANCER

By Erin L. Britt, B.S.

A thesis submitted in partial fulfillment of the requirements for the degree of Master of Science at Virginia Commonwealth University

Virginia Commonwealth University, 2018

Major Director: Hisashi Harada, Ph.D.
VCU School of Dentistry
Philips Institute for Oral Health Research

Head and neck cancer accounts for approximately 3 percent of all cancers in the United States, and over 90% of them are head and neck squamous cell carcinoma (HNSCC). Chemotherapeutic drugs that treat HNSCC can activate BCL-2 family dependent apoptosis. Pro-apoptotic NOXA induced by adenovirus (Ad-NOXA) or fenretinide inactivates anti-apoptotic MCL-1, while ABT-263 can inactivate other anti-apoptotic BCL-2 family members such as BCL-2 and BCL-X_L. We used p53 inactive HN8 and HN12, p53 wild-type UMSCC1, and HPV-positive UMSCC47 human HNSCC cell lines and five mouse HNSCC cell lines. Cells were treated with Ad-NOXA, ABT-263, and fenretinide alone or in combinations. Combinational treatment of ABT-263 with Ad-NOXA or fenretinide enhanced cell death among all cell lines we tested regardless of p53 status. These findings support the hypothesis that combinational treatment of Ad-NOXA or fenretinide with ABT-263 increases cell death by simultaneously inhibiting all anti-apoptotic BCL-2 family proteins in HNSCC cells.

Introduction

1.1 Cancer

Cancer is an extremely prevalent collection of diseases in the world and society, and it is the second leading cause of death in the United States^[1]. In 2018, the overall estimated new cases of cancer in the United States is 1,735,350, contributing to an estimated number of 609,640 deaths^[1]. Cancer is caused by genetic changes that can be inherited or arise during an individual's life. Additionally, different environmental exposures, such as radiation, ultraviolet rays, and chemicals from tobacco, can be cancer causing by contributing to DNA damage [www.cancer.gov]. Many other risk factors of cancer include age, alcohol, diet, obesity, and virus infection [www.cancer.gov].

There are many different types of cancer, and all cancers are characterized by uncontrolled cell growth [www.cancer.gov]. Cancer cells are different from normal cells because normal cells die when they get too old or damaged [www.cancer.gov]. Cancer cells do not die like normal cells, continuing to grow and divide.

Many cancer cells can form solid tumors, but there are types of cancer where this is not the case, such as leukemia, or cancer of blood cells [www.cancer.gov]. While leukemia is cancer that begins in blood cells, carcinoma is the type of cancer that is formed by epithelial cells, and it is also the most common type of cancer [www.cancer.gov]. The most common types of cancer estimated for 2018 include lung and bronchus, colon and rectum, prostate (men), breast (women), and oral cavity and pharynx^[1].

Due to the large number of deaths each year caused by cancer, as well as its severe impact on the world and United States, it is important to research cancer, cell death, and the molecular

mechanisms of tumorigenesis in order to develop proper understanding of cancer progression and successful treatment.

1.2 Head and Neck Cancer

Head and neck cancer is a type of cancer that normally begins in squamous epithelial cells of the head and neck that line moist, mucosal surfaces [www.cancer.gov]. Out of the total estimated new cases of cancer in 2018, approximately three percent of them are head and neck cancer^[1]. Over 90% of head and neck cancer is classified as head and neck squamous cell carcinoma (HNSCC)^[2], but rare forms of head and neck cancer can occur in the salivary glands that are not classified as carcinoma [www.cancer.gov]. It occurs in the oral cavity, pharynx, larynx, paranasal sinuses and nasal cavity, and salivary glands, which can be seen in Figure 1 [www.cancer.gov]. Head and neck cancer is among the most common forms of cancer in men, and men are twice as likely to be diagnosed than women^[1,3]. Additionally, individuals over the age of 50 are more likely to be diagnosed [www.cancer.gov]. There are many symptoms of head and neck cancer including a sore throat that persists, change in voice, and trouble swallowing [www.cancer.gov].

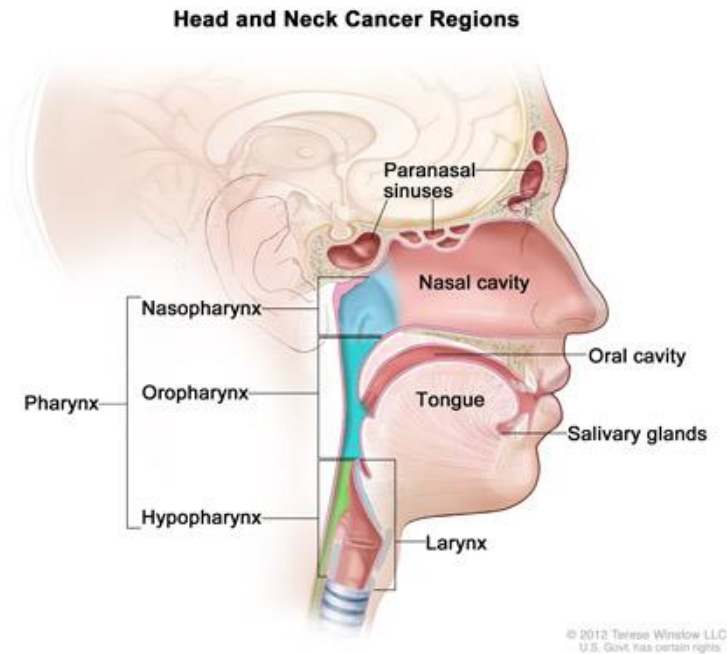


Figure 1: Locations of head and neck cancer [www.cancer.gov]

Head and neck cancer can arise from many different causes, similar to all cancers. However, the two main risk factors are use of alcohol and tobacco, chiefly for cancers in areas of the oral cavity, oropharynx, hypopharynx, and larynx^[3-5]. Seventy-five percent or more of head and neck cancer is caused by alcohol and tobacco^[4]. Additionally, those who use both alcohol and tobacco are more at risk for developing head and neck cancer than individuals who use either one^[4].

Another risk factor for developing head and neck cancer is human papillomavirus (HPV)^[2]. HPV describes over 200 viruses [www.cancer.gov]. Specifically, cancer of the oropharynx is strongly associated with HPV, and most cases of head and neck cancer associated with HPV are HPV-16 positive^[3,6]. It is known that the HPV virus encodes proteins E6 and E7, viral oncoproteins that interrupt tumor suppressor genes *p53* and *Rb*, respectively^[6]. While tobacco, alcohol, and HPV are mentioned as risk factors, there are a multitude of other risk factors

including poor oral health, radiation exposure, and occupational exposure such as exposure to wood dust [www.cancer.gov].

Staging of head and neck cancer involves understanding the location of the cancer and whether or not the cancer has spread to other parts of the body [www.cancer.net]. The stage of the cancer is determined by the Tumor-Node-Metastases (TNM) classification system and uses clinical, pathologic, and radiological examinations^[7]. The T determines size and degree of invasion of the primary tumor; the N classifies metastasis to the lymph nodes and size and location of lymph nodes affected, and the M describes if the metastasis has reached beyond the lymph nodes^[7]. Based on T, N, and M data the cancer is given a stage from I to IV^[7]. Stage I describes an earlier stage cancer that is minimally invasive, while Stage II and Stage III classify the cancer where a tumor has spread, possibly to the lymph nodes^[7]. Stage IV is the latest stage in which distant metastases has occurred^[7].

Treatment for head and neck cancer varies, depending on a variety of factors including classification and type of the cancer, age, and health [www.cancer.gov]. Early stages of head and neck cancer are curable, and treatment can be successful^[2]. However, little progress has been made over the past few decades for individuals with an advanced diagnosis^[2]. Main treatment options include surgery, radiation therapy, chemotherapy, targeted therapy, and combinational treatment [www.cancer.gov]. Treatment for an individual with head and neck cancer is normally determined by a group of specialized individuals from different disciplines^[8].

Surgery and radiation are treatment options that have been proven to cure certain cases of head and neck cancer^[8]. Additionally, since the 1990s, chemotherapy has been an accepted form of treatment and used in combination with radiation to increase cure rates^[8]. Other forms of treatment include immunotherapy and targeted therapy [www.cancer.net].

Some individuals with HNSCC may use a drug that targets a tumor protein called epidermal growth factor receptor (EGFR). Transforming growth factor alpha (TGF- α) and its receptor EGFR are elevated in individuals with HNSCC^[31]. Cetuximab targets EGFR and is an example of this class of drugs [www.onclive.com]. It is a monoclonal antibody that binds to the extracellular domain of EGFR^[32].

Immunotherapy is also a recent treatment modality for HNSCC, which targets the immune response to help identify and kill cancer cells. Checkpoint inhibitors inhibit cancer cell signaling by exposing them to T cells, which are adaptive immune cells [www.cancercenter.com]. Checkpoint inhibitors specifically target the programmed cell death protein-1 (PD-1) and cytotoxic T-lymphocyte-associated protein-4 (CTLA-4) receptors to help the immune system kill cancer cells [www.cancercenter.com].

Chemotherapy also kills cancer cells, and it is one of the most common treatments used for HNSCC [www.cancer.net]. Chemotherapy alone or in combination with surgery is not as effective as chemotherapy combined with radiation^[8]. Additionally, radiation and chemotherapy combination is the most common form of treatment for locally advanced HNSCC^[9]. Examples of chemotherapeutic drugs used for head and neck cancer are cisplatin, carboplatin, 5-fluorouracil, and taxanes^[9]. The mechanisms these drugs use are different and not fully understood, but each one induces cell death.

1.3 Cell death

Cell death occurs as a result of normal biological mechanisms and helps an organism maintain homeostasis^[10]. Cell death also plays an essential role in cancer^[10]. Apoptosis and necrosis are two of the major forms of cell death characterized by separate pathways^[10].

Autophagy, on the other hand, is known for its role in cell survival, but is also involved in the cell death process^[10].

Autophagy is a process used by cells for energy and recycling of nutrients, ultimately degrading cytosolic proteins and organelles^[10]. It typically occurs in response to stress, such as starvation, endoplasmic reticulum (ER) stress, or oxidative stress^[10]. If there is too much stress in the cell, non-apoptotic, type II cell death will occur by autophagy^[10]. It can be characterized by autophagosome formation and degradation by lysosomal hydrolases^[10].

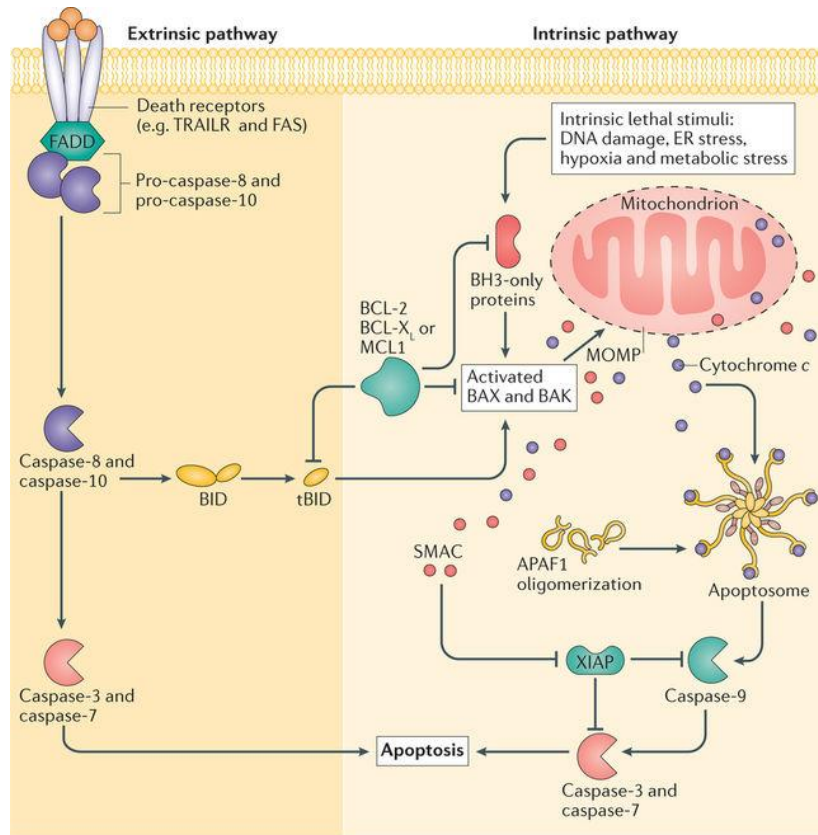
Necrosis is another type of cell death, which is defined as irreversible death of the body's tissue^[14]. Necrosis can be caused by injury, inadequate blood supply, chemicals, and radiation^[14]. It can be characterized by membrane degradation, leakage of intracellular material, and the inflammatory immune response^[14].

While necrosis is not actively controlled, apoptosis is highly regulated^[14]. It is a generally advantageous form of cell death that is known to play a role in embryonic development and adult homeostasis^[10, 11]. It is characterized by chromatin condensation, blebbing of the plasma membrane, and cleavage of cellular proteins^[10, 12]. Apoptosis is known to cause cell suicide following DNA damage, which can occur by chemotherapeutic drugs^[11]. This type of cell death requires the protease activity of caspases, which can occur through two separate pathways: the extrinsic or death receptor pathway and the intrinsic or mitochondrial pathway^[13] (Figure 2).

The extrinsic pathway is characterized by a death receptor family member. Examples of this are tumor necrosis factor (TNF)-related apoptosis-inducing ligand (TRAIL) receptor 1 (TRAILR1), TRAILR2, FAS, and TNF receptor 1 (TNFR1). The receptors are located at the plasma membrane and after ligand binding, the caspase cleavage cascade is activated, resulting

in cell death^[13]. Initiator caspases are caspase-8 and caspase-10, which cleave effector caspase-3 and caspase-7 and activate them^[13].

The intrinsic pathway is known to be deregulated in cancer and can be triggered by stressful stimuli including ER stress and DNA damage^[13]. It is characterized by mitochondrial outer membrane permeabilization (MOMP) and cytochrome *c* release into the cytosol from the intermembrane space (IMS)^[13]. The caspase cascade is activated through cytochrome *c* binding to adaptor molecule apoptosis protease activating factor 1 (APAF-1) and caspase-9, thereby forming a molecular complex known as the apoptosome^[12, 13]. After this, effector caspase-3 is cleaved and activated by caspase-9, resulting in cell death^[12]. For the regulation of cytochrome *c*, the BCL-2 family proteins play an essential role in this pathway^[15].



Nature Reviews | Cancer

Figure 2: Apoptosis signaling pathways ^[13]

1.4 BCL-2 Family members

The B-cell lymphoma-2 (BCL-2) family members are known to mediate the intrinsic apoptotic pathway in vertebrates^[15]. These family members can be divided into pro-apoptotic and anti-apoptotic (pro-survival) proteins. Most cells contain a variety of these proteins to regulate cell survival and cell death^[15].

All members of the BCL-2 family have a BCL-2 homology (BH) domain and can be further subdivided based on which BH domains they contain and function (Figure 3). The anti-apoptotic BCL-2 family proteins contain BH1, BH2, BH3, and BH4 domains and are normally localized at the outer mitochondrial membrane (OMM), but can also be in the cytosol or on the ER membrane^[15]. Members of this family include A1, BCL-2, BCL-X_L, BCL-w, and myeloid cell leukemia-1 (MCL-1) and protect the OMM by inhibiting pro-apoptotic BCL-2 family members^[15]. Pro-apoptotic BCL-2 family members are divided into multi-domain or effector proteins, and BH3 domain-only proteins^[15]. Effector proteins include BCL-2 homologous antagonist killer (BAK) and BCL-2 associated X protein (BAX), which contain BH1, BH2, BH3, and BH4 domains. BH3-only pro-apoptotic BCL-2 family proteins include BCL-2 antagonist of cell death (BAD), NOXA, BH3 interacting domain (BID), BCL-2 interacting mediator of cell death (BIM), and PUMA^[15, 16].

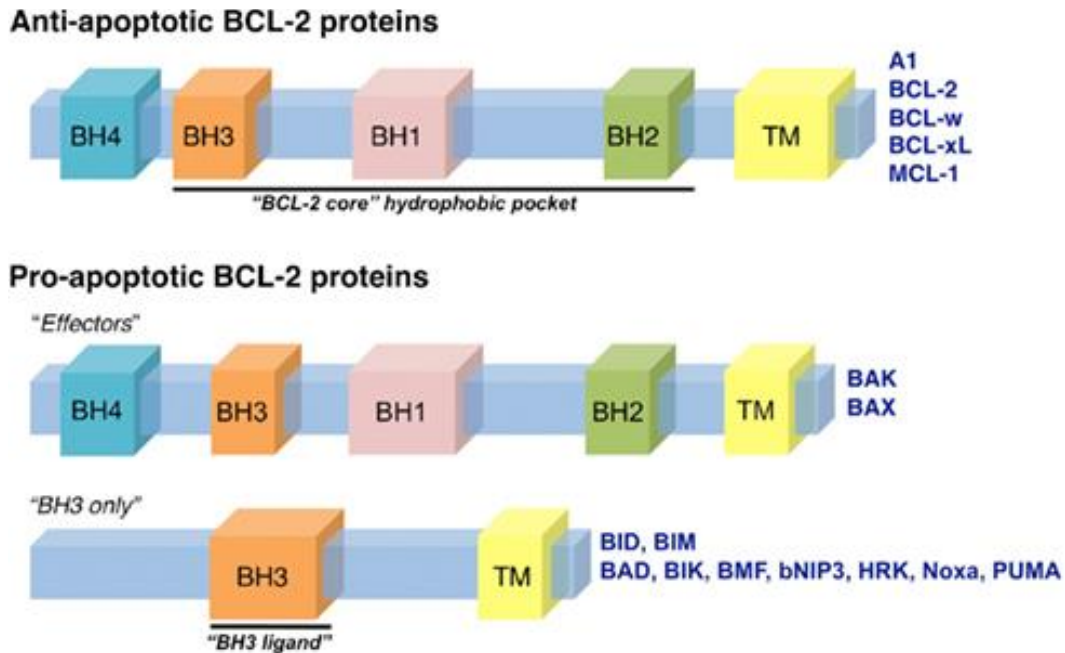


Figure 3: BCL-2 family members as defined by BH domains^[16]

While BID and BIM are known to directly activate BAK and BAX, the other BH3-only proteins can indirectly activate BAK and BAX and are known as “sensitizer” or “de-repressor” proteins that have different binding profiles (Figures 4A, 4B)^[15]. Sensitizer proteins form complexes with anti-apoptotic proteins that are already associated with effector proteins, allowing effector proteins to become released and activated^[15]. This may happen by induction of a de-repressor protein after cellular stress, where an anti-apoptotic protein is bound to an effector protein^[15]. For example, NOXA binds to the anti-apoptotic protein MCL-1, leading to its inactivation^[56]. Then, the effector protein can activate BAK or BAX, leading to apoptosis^[56]. Overall, BH3-only proteins can activate effector proteins to cause apoptosis, while anti-apoptotic proteins prevent this (Figure 5).

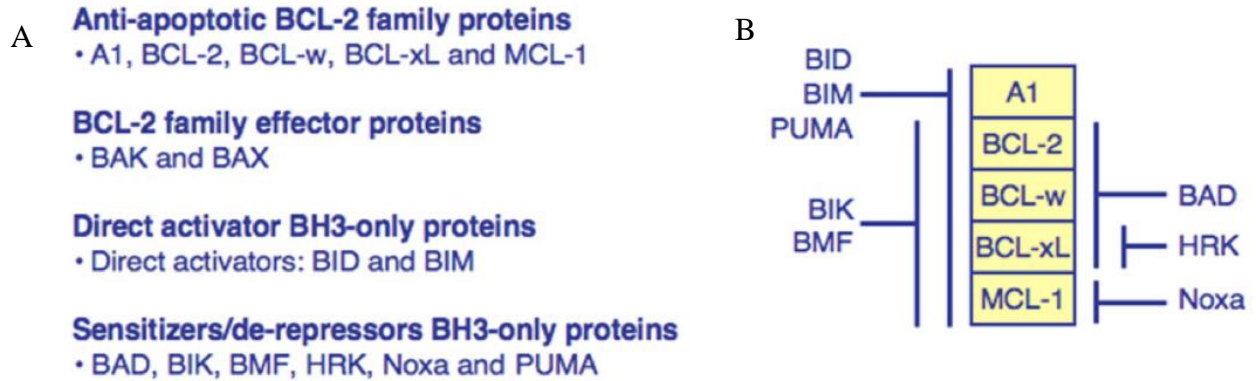
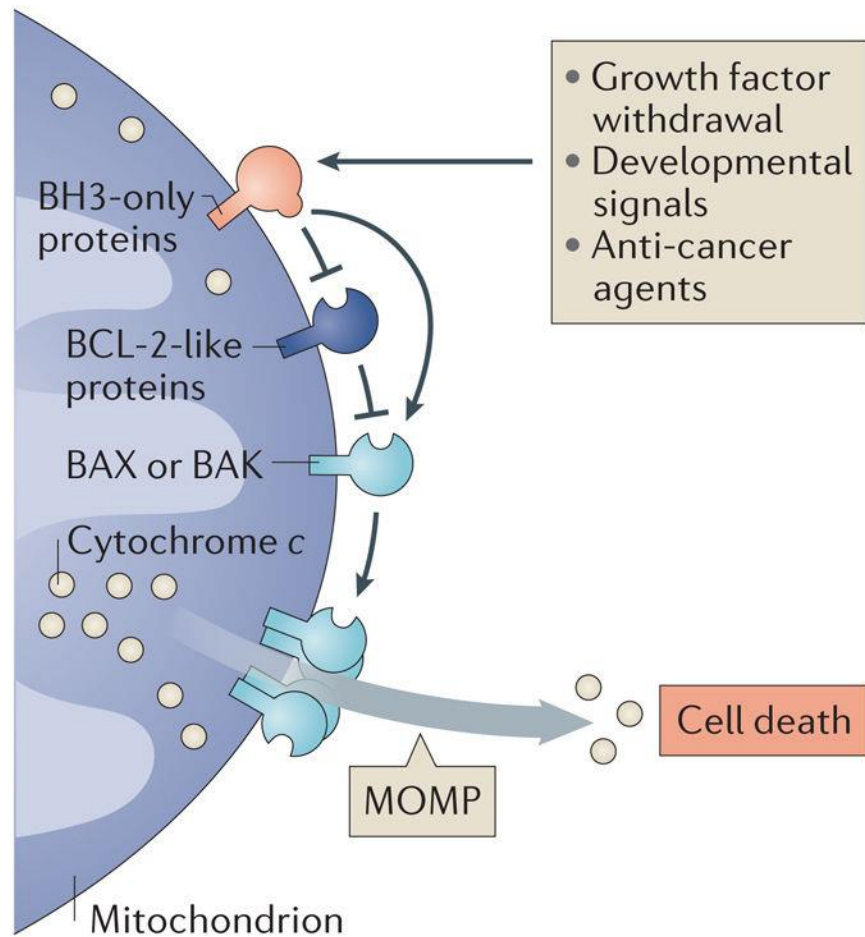


Figure 4: BCL-2 family members and function. A: BCL-2 family anti-apoptotic proteins and pro-apoptotic proteins defined as effectors, direct activators, and de-repressors. B: Binding profiles of anti-apoptotic BCL-2 family members^[15].

When cell death stimuli are elicited into the cell, mitochondrial apoptosis follows. The effector proteins BAX and BAK become activated by sensitizers, direct activators, or a combination. When BAX becomes activated, it translocates from the cytosol to the mitochondrial membrane, undergoing a conformational change^[56]. While the complete mechanism is not fully understood, it is also known that the C-terminus transmembrane domain inserts into the outer membrane of the mitochondria, and the N-terminus becomes exposed^[17, 18, 56]. BAK is already localized at the outer membrane of the mitochondria, but when it becomes activated, it also goes through a conformational change, exposing its N-terminus as well^[17]. When BAK or BAX become activated, they homo- or hetero-oligomerize to create a pore in the OMM, leading to MOMP, cytochrome *c* release into the cytosol, and cell death^[10, 15].



Nature Reviews | **Cancer**

Figure 5: BCL-2 family members mediate apoptosis in the mitochondrial pathway^[20]

1.5 Cisplatin

Cisplatin was discovered by Rosenberg and associates in 1965^[24]. They found that cell division in *Escherichia coli* (*E. coli*) cells near a platinum electrode could be prevented^[24]. Since then, this compound became a main player in a new class of chemotherapeutic drugs. Other platinum-based anticancer drugs include carboplatin and oxaliplatin^[26].

Cis-Diamminedichloroplatinum (II), which goes by the common name cisplatin, is a platinum-based compound that was approved for clinical use for testicular cancer in 1979^[23]. It is

currently used in combination with other drugs or alone for many cancers including bladder cancer, ovarian cancer, testicular cancer, HNSCC, and non-small cell lung cancer^[26]. It is the most common type of chemotherapeutic drug used for HNSCC [www.headandneckcancerguide.org]. Cisplatin treatment can be limited due to toxicity and development of resistance^[27].

The molecular structure of cisplatin is $\text{Pt}(\text{NH}_3)_2\text{Cl}_2$ (Figure 6), and *in vitro* models have proven that the positions of chloride and ammonia groups are required to be “cis” in order to function clinically^[25]. Additionally, cisplatin can cross-link with DNA, most often between guanine-guanine groups, causing DNA damage^[25]. This leads to the inhibition of replication and the cell death response. The particular mechanism of action involves a nucleophilic substitution reaction, where one chlorine atom is replaced by a hydroxyl group, and a covalent bond between DNA and cisplatin is formed (Figure 7). The reaction of cisplatin inside the cell is an aquation reaction, and cisplatin binds to the N⁷ guanine position, forming either a 1,2- or 1,3-intrastrand crosslink.

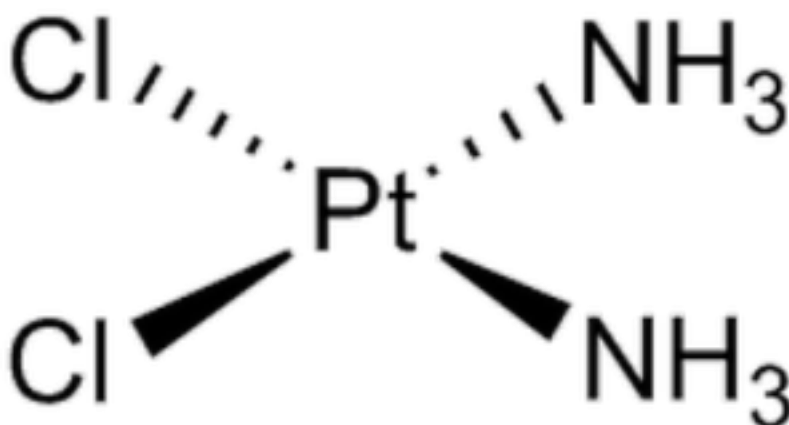


Figure 6: Molecular structure of Cisplatin

<http://www.jmfinechemicals.com/product/cisplatin-2/>

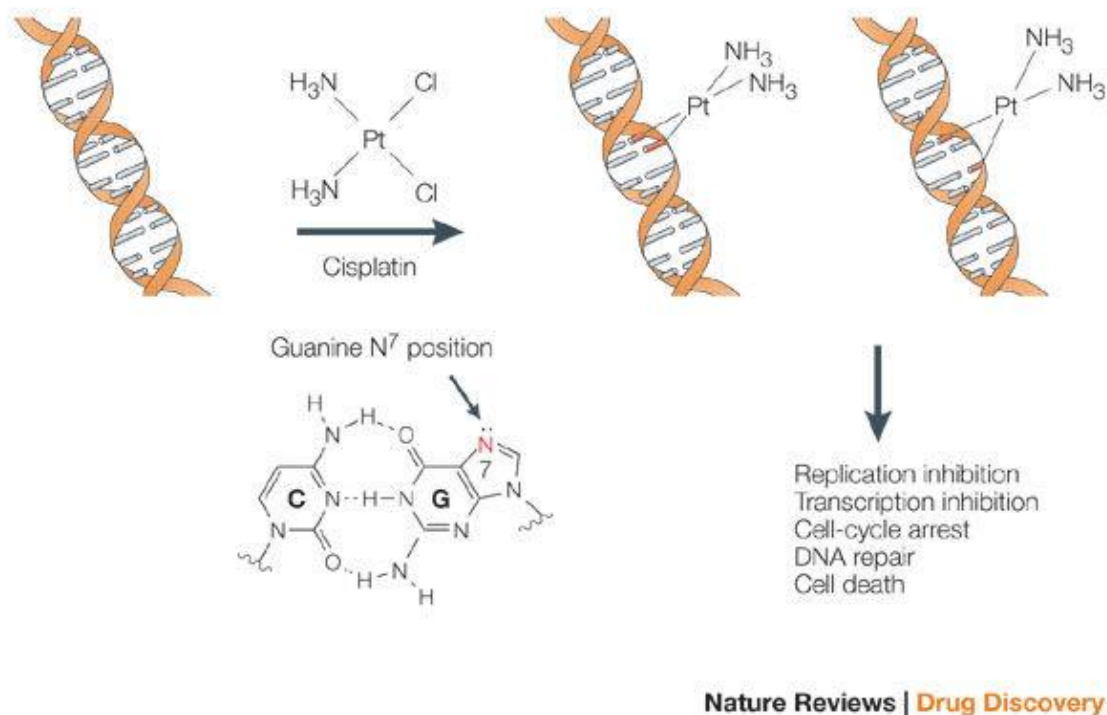


Figure 7: Mechanism of action of Cisplatin^[28].

Cisplatin is known to lead to apoptosis through the BCL-2 family-pathway, and in particular, the transcription of NOXA is induced^[26]. NOXA induces cell death by MCL-1 degradation and MCL-1 phosphorylation occurs prior to degradation^[27]. Specifically, phosphorylations at sites Ser64 and Thr70 occur on MCL-1^[27]. Regulation of phosphorylation requires that MCL-1 and CDK2 (cyclin dependent kinase 2) form a complex. When NOXA binds to this complex, phosphorylation is enhanced^[27]. Thus, a major regulatory mechanism is facilitated by the NOXA, MCL-1, CDK2 complex^[27]. Ultimately, it was found that the induction of NOXA by cisplatin was essential for apoptosis, and this occurs in a p53-independent manner^[30]. It was further identified that ATF3 and ATF4 play a role in the regulation of *Noxa* mRNA induction by cAMP response element (CRE) on the *NOXA* promoter when cisplatin was treated^[30]. While NOXA is induced by cisplatin in a p53-independent manner, it has also been found that cisplatin

can induce apoptosis in a p53-dependent manner because it was originally discovered that NOXA was a p53 target gene.

1.6 p53

p53 is a tumor suppressor protein that serves as a transcriptional regulator in response to DNA damage^[8] and causes both DNA repair and apoptosis^[10, 21]. When cells are damaged, ataxia telangiectasia mutated (ATM) and ataxia telangiectasia and Rad3-related (ATR) kinases are activated, phosphorylating p53 and mouse double minute 2 homolog (MDM2), disrupting the p53 and MDM2 interaction^[10]. MDM2 binds to the N-terminal transactivation domain of p53 and serves as an E3 ubiquitin ligase, functioning to degrade p53^[57]. When the interaction between p53 and MDM2 is interrupted, p53 is stabilized. From here, p53 is upregulated, activating many proteins involved in apoptosis and cell regulation^[10, 21].

When DNA damage occurs, p53 can induce a CDK inhibitor p21, cause G1 arrest in the cell cycle, repair the DNA, and resume cell division^[8]. However, if the cell undergoes DNA damage that is detected by the cell as too much, apoptosis can be initiated by p53^[8]. p53 is mutated or deleted in many cancers because it plays a key role in cell cycle regulation, apoptosis, and DNA repair^[10]. In HNSCC, p53 mutations are among the most common genetic alterations^[22]. The most common mutation occurs in the DNA binding domain due to a missense mutation^[21], rendering it inactive as a transcription factor^[10]. Because p53 mutations are common in cancer, there is development of p53-independent mechanisms of treatment.

1.7 NOXA and MCL-1

Cisplatin was found to induce NOXA in both p53-dependent and p53-independent manners^[27, 57]. NOXA is a BH3-only BCL-2 family member that is involved in the mitochondrial apoptotic pathway. In 1990, Hijikata and associates cloned the first *Noxa* cDNA from an adult T-cell leukemia (ATL) library, and its transcript was induced by phorbol 12-myristate 13-acetate (PMA) treatment in Jurkat T-cell acute lymphoblastic leukemia, peripheral blood mononuclear cells, and embryonic lung cells^[33]. Therefore, it was given the name ATL-derived PMA responsive gene (APR)^[33]. It was then named PMA-induced protein 1 (PMAIP1), but the function of this protein remained unknown for another 10 years^[34].

The protein was rediscovered in mouse embryonic fibroblasts when it was found that cDNA encoded a 103-amino acid protein and was named NOXA, which is Latin for damage^[34]. It was revealed that NOXA contained only a BH3 domain, categorizing it as a BH3-only BCL-2 family member^[35]. It was also found that the structures of mouse and human NOXA are different because mouse NOXA is approximately twice as long as the human isoform and has two BH3 domains (Figure 8)^[34]. Both mouse and rat NOXA contain three exons, which is the same number for humans^[34].

		BH3 domain			
		A motif			
mouse Noxa	1	MPGRKARRNAPVNPTRAE	LPPEFAAQ	LRKIGDKVYCTWSAPDITV	VVLAQMPG 53

rat Noxa	1	MPGRKARRNAPLNPTRAE	LPPEFAAQ	LRKIGDKVYCTWSAPDITAV	VLAQMPG 53
		***	***	***	***
human Noxa	1	MPGKKARKNAQPSPARA			17
		BH3 domain			
		B motif		MTD	
mouse Noxa	54	K-SQKSRMR-SPSPTRVPADL	KDECA-Q	LRRIGDKVNL	RQKLLNLI SKLFNLVT 103
		*		*	*
rat Noxa	54	KKSRKSTMRRSPSPTRVPADL	KDECD-Q	LRRIGDKVNL	RQKLLNFI SKLFNLIT 105
		**	*	*	*
human Noxa	18	PAELEVECATQ	LRRFGDKLN	FRQKLLNLI	SKLFCSGT 54

Figure 8: Sequences of human, rat and mouse NOXA^[34]. The mitochondrial targeting sequence (MTD) and BH3 domains are shown.

NOXA is the smallest of the BH3-only BCL-2 family proteins with just 54 residues in human and selectively interacts with the anti-apoptotic BCL-2 family member MCL-1 to cause apoptosis^[34]. DNA damage can cause NOXA to induce apoptosis. NOXA-induced apoptosis requires a functional BH3 domain, and overexpression causes NOXA to localize to the mitochondria by its MTD^[35, 36]. Then, NOXA becomes ubiquitinated on lysine residues and MCL-1 is recruited to the mitochondria from the cytosol by binding to NOXA's BH3 domain^[36]. MCL-1 and CDK2 form a complex, and CDK2 facilitates the phosphorylation of Ser64 and Thr70, which is required for MCL-1 ubiquitination (Figure 9)^[27]. From here, MCL-1 is degraded and apoptosis follows.

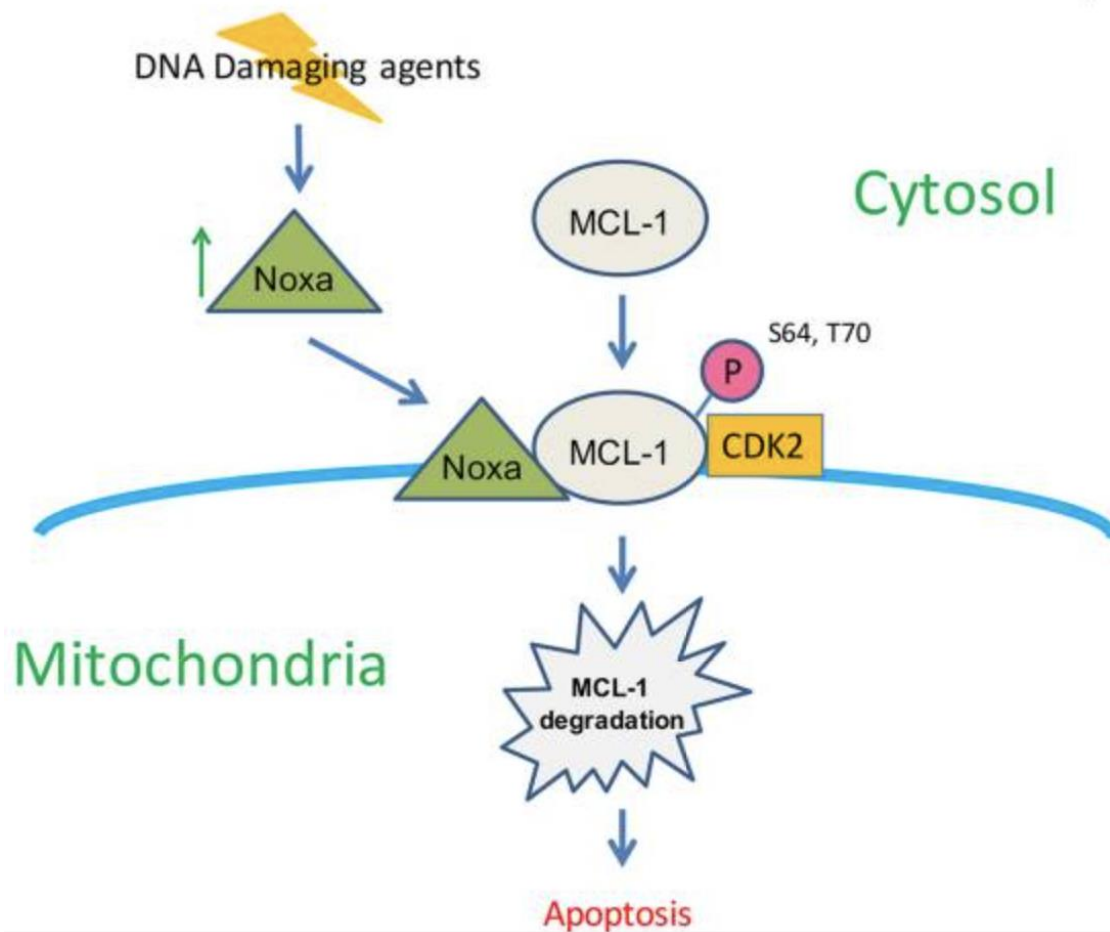


Figure 9: Mechanism of NOXA induction leads to apoptosis ^[27]

MCL-1 is an anti-apoptotic protein that was identified during PMA-induced differentiation of myeloid leukemia cells in 1993^[37]. It was identified as a BCL-2 family member, being the second protein to be discovered in that family^[38]. MCL-1 contains three BH domains and is notably different from other BCL-2 family members in structure because it consists of 350 amino acids^[38]. Other large BCL-2 family members are BCL-2, which is 139 amino acids and BCL-X_L, which is 233 amino acids. MCL-1 contains a hydrophobic groove on its surface for the binding of other proteins with BH3 domains^[39]. Its anti-apoptotic function comes from its binding to BAK, which sequesters and inhibits the apoptotic function^[38]. MCL-1 has a N-terminus portion

that is not homologous with the BCL-2 family and plays a large role in its function and regulation through changes in stability, transcription, and localization^[38]. Kozopas and associates identified the region as rich in Proline (P), Glutamic acid (E), Serine (S), and Threonine (T) residues, which causes a short half-life of MCL-1 and is named the PEST region^[37].

MCL-1 can be activated by many survival and differentiation signals and its expression is controlled at transcriptional, post-transcriptional, and post-translational levels^[41]. The phosphorylation of glycogen synthase kinase 3 (GSK-3) at multiple residues is key to MCL-1 degradation^[38]. However, extracellular signal-related kinase 1 (ERK1) phosphorylation at Threonine 163 stabilizes MCL-1^[38]. As is the case of DNA damaging agents where MCL-1 can be translocated by NOXA, causing its degradation and apoptosis for the cell, MCL-1 can be cleaved and inactivated by caspases, leading to apoptosis as well^[30, 42]. There are many chemotherapeutic drugs that target NOXA, leading to the degradation of MCL-1 and the apoptotic pathway. Cisplatin is a FDA-approved drug that has been shown to induce NOXA and fenretinide is a drug currently in many clinical trials that has also been shown to induce NOXA.

1.8 Fenretinide

Fenretinide is an orally available analogue of retinol (Vitamin A) that is currently used in clinical trials due to its antineoplastic and chemopreventative actions [www.cancer.gov]. It is different from other naturally occurring retinoids because it does not induce systemic catabolism, which would interfere with regulation of plasma levels with long-term usage [www.cancernetwork.com]. Other unique biologic effects of fenretinide are production of reactive oxygen species (ROS) and lipid second messengers that may be involved in cell death

induction of transformed, premalignant, and malignant cells^[43]. Additionally, fenretinide has low toxicity and the ability to arrest tumorigenesis [www.cancernetwork.com].

Fenretinide's chemical name is N-4(-hydroxyphenyl)retinamide, and its structure can be seen in Figure 10. It is known to activate retinoic acid receptors (RARs) and subsequently induce cell differentiation and cell death in cancers [www.cancer.gov]. It can also induce cell death in tumor cells by regulating growth factors associated with angiogenesis that is RAR-independent [www.cancer.gov]. It has been shown to kill cancer cells *in vitro* and *in vivo*^[44-48]. In animal models, fenretinide has shown anti-cancer effects in breast, skin, pancreas, and prostate tumorigenesis^[45, 46]. It has also been shown to slow prostate cancer progression in men and breast cancer in women^[47, 48]. Additionally, fenretinide can induce apoptotic cell death in HNSCC cells at doses that are clinically relevant^[44].

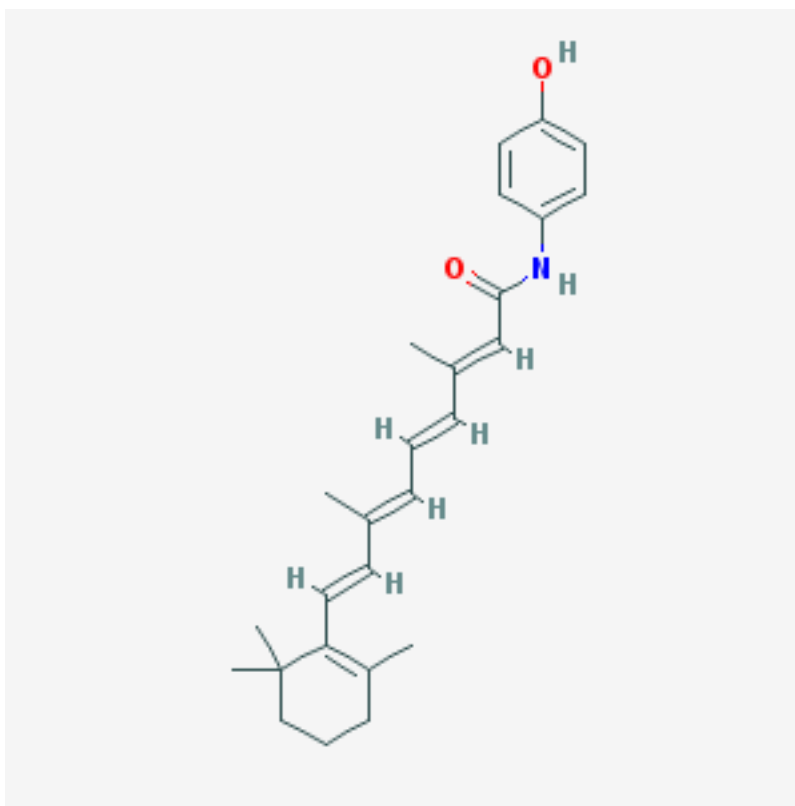


Figure 10: Chemical structure of Fenretinide

[<https://pubchem.ncbi.nlm.nih.gov/image/imgsrv.fcgi?cid=5288209&t=1>]

Fenretinide has been shown to induce ER stress through a RAR-independent pathway in neuroblastoma and melanoma cells^[49]. When these cells were treated with fenretinide, the eukaryotic initiation factor 2 alpha (eIF2 α)-ATF4 signaling pathway mediated ER-induced apoptosis^[49]. When eIF2 α signaling was induced by fenretinide, there was subsequently increased expression of eIF2 α , ATF4, ATF3, and GADD34 and induction of NOXA^[49]. When NOXA is induced, MCL-1 is sequestered and inactivated and apoptosis ensues^[50].

1.9 ABT-263 (Navitoclax)

While Fenretinide can inactivate the anti-apoptotic protein MCL-1, ABT-263 can inactivate other anti-apoptotic proteins. ABT-263 is a BH3 mimetic drug that is orally available and inhibits BCL-2, BCL-X_L, and BCL-w function so that apoptosis can occur^[51]. It is currently undergoing many clinical trials due to its pro-apoptotic activity in many cancer cell types, and most notably in small cell lung cancer (SCLC)^[53]. ABT-263 prevents the binding of BCL-2 and BCL-X_L to BAK and BAX, triggering cell death [www.cancer.gov].

ABT-737 is a prototype of ABT-263, but its chemical properties make it difficult for use as a chemotherapeutic agent, as it is not orally available and has low aqueous solubility^[51]. This is why ABT-263 has been synthesized so that it can be used orally and as a single agent^[51]. To produce ABT-263, scientists identified key sites on ABT-737 that needed to be modified because they effected oral absorption, metabolism, and charge balance (Figure 11)^[51]. ABT-263 incorporated these factors and the sites were modified (Figure 11)^[51].

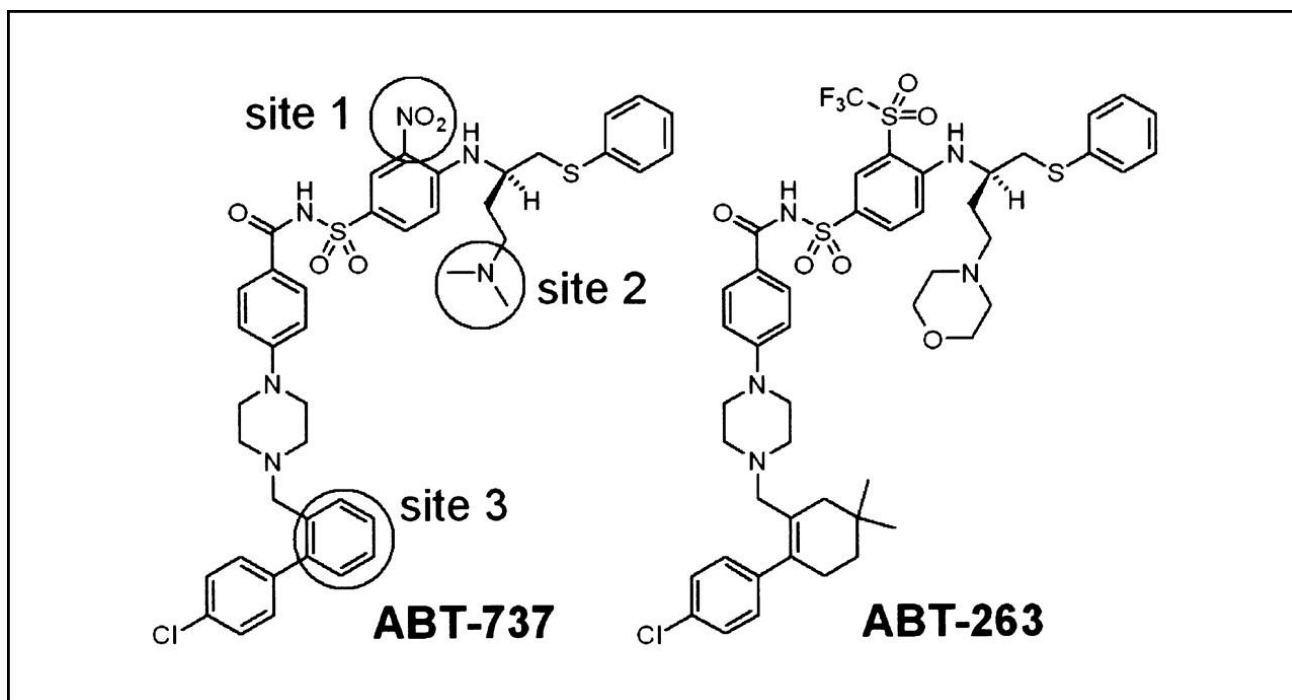


Figure 11: Chemical structures of ABT-737 and ABT-263^[51]

The mechanism of ABT-263 has been proven to exhibit cytotoxicity to cancer cells by inhibiting BCL-2 family members BCL-2 and BCL-X_L through protein-protein interactions^[51]. The particular protein-protein between anti-apoptotic proteins to pro-apoptotic proteins are between the hydrophobic groove of the anti-apoptotic protein and BH3 domain of its partner^[54]. ABT-263 interrupts this interaction so that the hydrophobic groove of the anti-apoptotic protein is now bound to ABT-263^[55]. As a small-molecule inhibitor, ABT-263 targets the BH3 domain interaction, and this is why it is called a BH3 mimetic chemotherapeutic drug^[55]. Immunoprecipitation studies found that BIM and BCL-X_L interaction was decreased with ABT-263, as well as BIM and BCL-2 interaction^[53]. However, it was shown that ABT-263 did not inhibit the anti-apoptotic protein MCL-1^[53].

ABT-263 has been proven to exhibit cytotoxicity to SCLC cells *in vitro* and *in vivo*^[51]. It has also been shown that dose increase can induce thrombocytopenia, reducing circulating platelets^[52]. However, this effect can be reversible and monitored^[51]. The effects of ABT-263

are significant both as a single agent and combined with chemotherapy^[51]. Faber and associates assessed the sensitivity of ABT-263 across over 500 cell lines and found that those with high BIM expression were sensitive to ABT-263, making SCLC cells one of the most sensitive to this drug^[53]. However, ABT-263 did not have cytotoxic effects on cancer cells that had high levels of MCL-1^[53]. In cancers with expression of MCL-1, it could be useful to combine NOXA-inducers with ABT-263 to inhibit all anti-apoptotic BCL-2 family members. For example, fenretinide and ABT-737 exhibited synergistic effects in melanoma. This drug combination resulted in induction of NOXA and caspase-dependent degradation of MCL-1^[50].

Hypothesis

Cisplatin is a FDA-approved chemotherapeutic drug for HNSCC that has been proven to induce NOXA, a pro-apoptotic BCL-2 family member and lead to cell death through the apoptotic pathway. NOXA binds to MCL-1, leading to its inactivation and degradation, causing BAK to be activated and released. Additionally, fenretinide is known to induce NOXA through ER stress to similarly inactivate MCL-1. While NOXA-inducing drugs can inhibit MCL-1, ABT-263 can inactivate other anti-apoptotic family members such as BCL-2 and BCL-X_L. **We hypothesize that the induction of NOXA in HNSCC cells in combination with ABT-263 treatment will efficiently induce apoptosis by simultaneously inhibiting all pro-survival BCL-2 family proteins.**

Specific Aims

3.1 The first aim is to determine the underlying molecular mechanisms of cell death induced by Adenovirus-mediated NOXA expression (Ad-NOXA) or Ad-NOXA with ABT-263 combination treatment.

Cell death was analyzed by Western Blot and fluorescence activated cell sorting (FACS) analyses through Annexin V- Propidium Iodide (PI) staining. The lentiviral short-hairpin BAK (shBAK), BAX (shBAX), and BIM (shBIM) were introduced into HNSCC cells to determine involvement of these BCL-2 family members in Ad-NOXA-induced cell death.

Immunoprecipitation experiments were done with MCL-1 and BAK to determine the BCL-2 family member interactions when NOXA was overexpressed.

3.2 The second aim is to determine the underlying molecular mechanisms of cell death induced by Fenretinide or Fenretinide with ABT-263 combination treatment.

Cell death was analyzed by Western Blot and FACS analyses through Annexin V-PI staining.

Materials and Methods

4.1 Cell lines and cell culture

HN8 and HN12 were provided by Dr. W. Andrew Yeudall (Augusta University). UMSCC1 was provided by Dr. Yue Sun (Virginia Commonwealth University), and UMSCC47 was provided by Dr. Iain Morgan (Virginia Commonwealth University). Mouse cell lines 601, 602, 604, 606, and 613 was established by Dr. Hisashi Harada by extracting tumors from mice tongues. Four to six-week-old female C57BI/6 mice were given 50 µg/ml of 4-nitroquinoline oxide (4NQO) into their drinking water for 16 weeks. The 4NQO mouse model is well known, causing preneoplastic histological changes that come from DNA damage and genetic mutations^[29]. 4NQO mimics human exposure to tobacco carcinogens and causes tumor formation in the oral cavity^[29]. Once tumors formed, they were excised and cultured into 5 different cell lines from five different mice.

HN8, HN12, UMSCC1, and UMSCC47 were cultured in Dulbecco's Modified Eagle Medium (DMEM) (Life Technologies) and supplemented with 10% heat-inactivated fetal bovine serum (FBS) (Gemini Bio-Products, West Sacramento, CA) and 100 µg/mL penicillin G/streptomycin (Invitrogen) at 37°C in a humidified, 5% CO₂ incubator. 601, 602, 604, 606, and 613 were cultured in RPMI 1640 medium with addition of 10% heat-inactivated fetal bovine serum (FBS) (Gemini Bio-Products, West Sacramento, CA) and 100 µg/mL penicillin G/streptomycin (Invitrogen) at 37°C in a humidified, 5% CO₂ incubator. 293T cells were purchased from American Type Culture Collection (Manassas, VA).

4.2 Adenovirus production

NOXA-expressing adenovirus (Ad-NOXA) was constructed by inserting Flag-tagged NOXA cDNA into pAdTrack-CMV vector (Addgene, Cambridge, MA), while the control adenovirus contained the vector alone. The adenovirus could then be used for treatment in human and mouse cell lines.

4.3 Lentivirus production

Lentiviral short-hairpin RNA (shRNA) expressing constructs were purchased from Sigma-Aldrich (St. Louis, MO) or Open Biosystems (Huntsville, AL). Constructs were transfected with packaging plasmids (Addgene, Cambridge, MA) into 293T packaging cells with EndoFectin Lenti (GeneCopoeia, Rockville, MD) and the supernatants containing the lentivirus were collected. The cell line of interest was seeded in a 6-well plate and the media was removed the next day. Then, 1 mL of media and 1 mL of supernatant containing the lentiviruses were added into each well with 2 μ L of 10mg/mL polybrene. After this, the 6-well plate was spun down in a centrifuge at 2000 rpm for 1 hour to allow the viruses to bind to the cells. Stable cell lines were established by puromycin (2 μ g/mL) selection.

4.4 Antibodies and Chemicals

Fenretinide and ABT-263 were purchased from ApexBio Tech (Houston, TX). Antibodies for BIM, BAK, PARP, Cleaved PARP (Asp214), GAPDH (D16H11), MCL-1 (for mouse cells), HRP-linked anti-rabbit IgG, HRP-linked anti-mouse IgG, and Anti-Rabbit IgG conformation-specific were from Cell Signaling Technology (Beverly, CA); NOXA (114C307.1) was from Thermo Fisher Scientific (Waltham, MA); MCL-1 (ADI-AAP-240-F) was from Enzo Life Sciences (Farmingdale, NY). ECL2 Western blotting substrate (80196) was purchased from

Thermo Fisher Scientific (Rockland, IL). Annexin V-APC was purchased from Invitrogen by Thermo Fisher Scientific (Waltham, MA). Propidium Iodide was purchased from Sigma Aldrich (St. Louis, MO).

4.5 Western blot analyses

Whole HNSCC cell lysates were prepared with CHAPS lysis buffer [20 mM Tris (pH 7.4), 137 mM NaCl, 1 mM dithiothreitol (DTT), 1% CHAPS (3-[(3-Cholamidopropyl)dimethylammonio]-1-propanesulfonate)], 1:200 ratio of protease inhibitor cocktail, and 1:100 ratio of phosphatase inhibitor cocktails 2 and 3 (Sigma-Aldrich, St. Louis, MO)]. Protein concentrations were determined by the Bradford method on a spectrophotometer (Bio-rad, Hercules, CA), and equal amounts were loaded onto SDS-polyacrylamide gels. The gel was run at 180 Volts for approximately 45 to 60 minutes. Then the gels were transferred onto nitrocellulose membranes (Fisher Scientific, Pittsburgh, PA) at 100 Volts for 60 minutes. Blocking occurred as the next step for approximately 30 minutes with a blotting solution [5% skim milk in PBST (1 x PBS with 0.1% Tween-20)]. Specific primary antibodies were incubated overnight at 4°C. The next day, the membrane was washed with PBST for five minutes in three separate washes and then incubated with a secondary antibody for one hour at room temperature. The secondary antibodies were either HRP-linked anti-rabbit IgG or anti-mouse IgG antibodies. The last step is development using ECL-2 Western Blotting Substrate (Thermo Fisher Scientific).

4.6 Fluorescence Activated Cell Sorting (FACS) analyses

Human HNSCC cells (1×10^5) or 2×10^5 mouse HNSCC cells per well in 1mL of medium were seeded in a 12-well plate and treated with Ad-NOXA, fenretinide (10 μ M), ABT-263 (1 μ M for human cells and 0.5 μ M for mouse cells), or in combination. The control was treated with control adenovirus. Cells were trypsinized 24 hours later and spun down for two minutes at 8000 rpm. The supernatant was aspirated and pellets were suspended with 1mL of cold 1 x PBS. This was spun down again for two minutes at 8000 rpm, and each pellet was suspended with 100 μ L of 1 x Binding Buffer [10mM Hepes (pH 7.4), 140mM NaCl, and 2.5mM CaCl_2] and transferred to a 5mL polystyrene tube. Then, 13 μ L of propidium iodide (10 μ L)-Annexin V APC (3 μ L) was added to each tube. In order to avoid bleaching the dyes, the tubes were left in the dark for 15 minutes. After 15 minutes, 400 μ L of 1 x Binding Buffer was added to each tube, and flow cytometric analysis was done using FACScan (BD Biosciences, San Jose, CA).

4.7 Crystal Violet assay

Cells were seeded in microtiter plates (96 wells) with 1×10^4 cells per well in 100 μ L of medium. On the following day, cells were treated with combinations of Ad-NOXA and fenretinide with ABT-263. After 72 hours, the media was aspirated and 100 μ L of 10% Buffered Formalin Phosphate solution (Fisher Scientific, Hampton, NH) was added to each well for 10 minutes. Then, the solution was aspirated and 100 μ L of 0.05% Crystal Violet Gram Stain (Fisher Scientific, Hampton, NH) was added. After approximately 30 minutes, the wells were washed with distilled water and dried.

4.8 Immunoprecipitation analysis

Whole HNSCC cell lysates were prepared with CHAPS lysis buffer. Equal amounts of protein were incubated with appropriate antibodies at 4°C overnight. Then the antibody complexes were captured with protein A/G beads (Pierce, Rockford, IL) at 4°C for 1 hour. After washing three times with CHAPS lysis buffer at 8000 rpm for 15 seconds, the beads were re-suspended in the same wash and loaded onto a SDS-polyacrylamide gel. The procedures of Western blot is described in the above section (Section 4.5). If the protein of interest was around 25 or 50 kD, the membrane was incubated with an anti-rabbit IgG conformation-specific antibody. Then, the membrane was washed three times in PBST for approximately 5 minutes each wash. After this wash, the secondary antibody was added. Secondary antibodies were either HRP-linked anti-rabbit IgG or anti-mouse IgG antibodies.

4.9 Statistical Analyses

The mean is represented in bar graphs, and standard deviation are indicated through the error bars in the graph (Mean \pm standard deviation). P-values were calculated using t-test in order to determine the statistical significance of data. P-values less than 0.05 indicate that the results are statistically significant.

Results

The results presented below clarify the aims of this project in association with each result.

5.1 Human HNSCC cell lines and characteristics

The human HNSCC cell lines and important characteristics are located in Figure 12. HN8 and HN12 originate from the lymph node and this means they are post-metastatic. In HN8, the patient's pre-metastatic cells are from the epiglottis. In HN12, the patient's pre-metastatic cells are from the base of tongue. The *p53* gene is deleted in HN8 and truncated in HN12. A point mutation was found in HN12 cDNA at the exon 7 splice donor site^[59], which is why there is lack of a band at 53 kDa in Western blotting (Figure 12, Right). Additionally, UMSCC47 and UMSCC1 possess wild-type (WT) *p53*. Additionally, the HPV status is negative in all human cell lines used, except for UMSCC47. It is HPV-16 positive [www.sigmaaldrich.com] and this is important because HPV encodes viral oncoprotein E6, which interrupts *p53* function^[6].

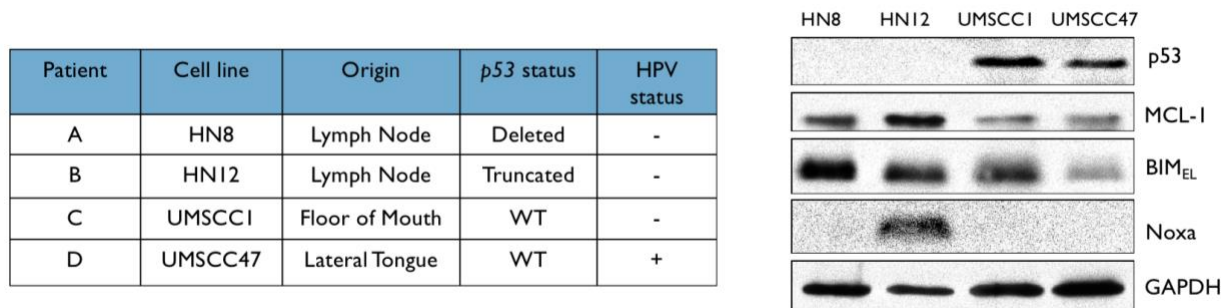


Figure 12: Human HNSCC cell lines and characteristics. Left: Chart characterizing the cell origin, *p53* status, and HPV status for each human HNSCC cell line. **Right:** Western blot of HN8, HN12, UMSCC1, and UMSCC47 untreated cells. Cells were seeded in a 6-well plate and harvested overnight. Equal amounts of samples were analyzed with the antibodies indicated in this figure.

Figure 12 also shows MCL-1, BIM_{EL}, and NOXA levels in HNSCC cell lines. The MCL-1 level appears to be higher in HN12 and lower in UMSCC1 and UMSCC47. Additionally, BIM_{EL}, (BIM extra-large, the most abundant isoform of BIM^[58]), is lower in UMSCC47 compared to other cell lines. Also, the level of NOXA is highest in HN12. GAPDH was used to confirm equal loading of cell lysates.

5.2 Ad-NOXA alone or Fenretinide alone can induce cell death in HN8

To examine the reaction of HN8 to drug treatment by Western blot, cells were seeded in a 6-well plate and treated with Ad-NOXA, fenretinide (10 μ M), ABT-263 (1 μ M), or combinations (Figure 13, Left). The control was treated with control adenovirus (vector alone). The cells were harvested overnight and the lysates were probed with cleaved PARP, MCL-1, BIM, NOXA, and GAPDH. Cleaved PARP is an indicator of apoptosis because PARP cleavage occurs by caspase-3 during the mitochondrial apoptotic pathway.

Similar analysis was done using FACS to determine the amount of cell death that was qualitatively assessed in the Western blot. For FACS, HN8 cells were seeded in a 12-well plate and treated in duplicates with control adenovirus, Ad-NOXA, fenretinide (10 μ M), ABT-263 (1 μ M), or combinations (Figure 13, Top Right). After 24 hours, cells were trypsinized and FACS analysis was performed.

HN8 has a certain amount of cell death when treated with Ad-NOXA or fenretinide alone. This can be confirmed through both Western blot and FACS analysis (Figure 13). The Western blot shows increased cleaved PARP with single treatment. However, combinational treatments of Ad-NOXA or Fenretinide with ABT-263 appear to increase cell death even more, as indicated by cleaved PARP. FACS analysis is consistent with this result as well. However, the

effect appears to be additive, rather than synergistic. Additionally, the Western blot shows that NOXA is highly expressed by Ad-NOXA and is strongly induced by fenretinide treatment.

To confirm that combinational treatment can completely kill HN8 cells, crystal violet assays were performed (Figure 13, Bottom Right). The crystal violet staining shows that cells have completely died with combinational treatment by the 72-hour point.

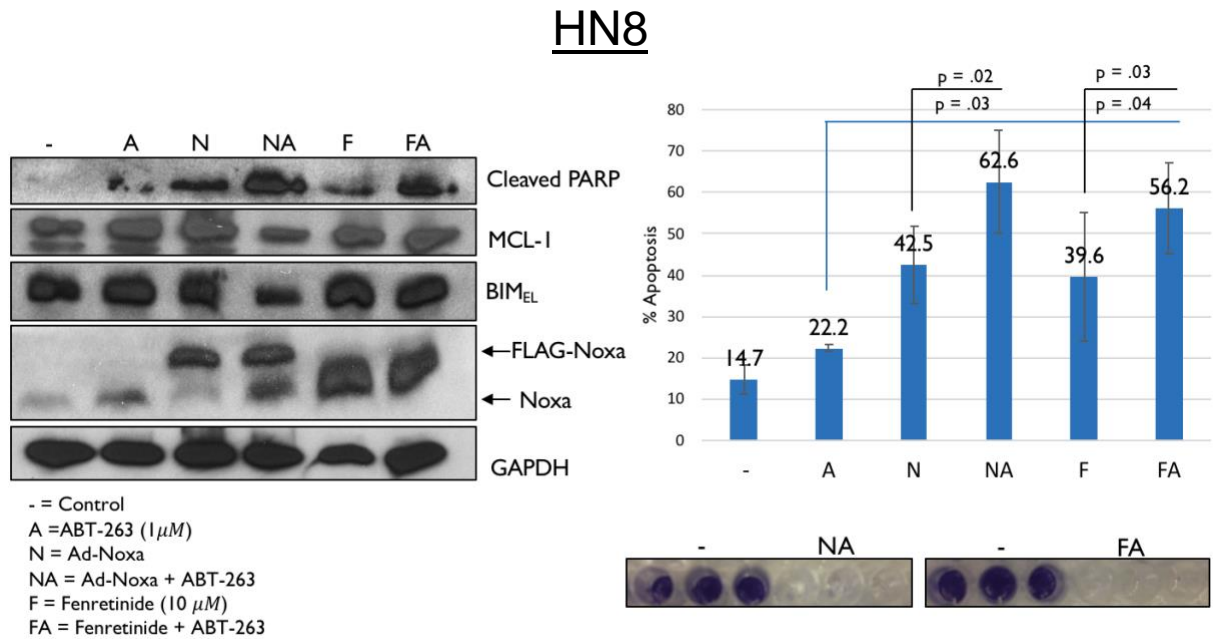


Figure 13: Ad-NOXA alone or Fenretinide alone can induce cell death in HN8. **Left:** Cells were treated with indicated drugs overnight and samples were analyzed by Western blotting with cleaved PARP, MCL-1, BIM, NOXA, and GAPDH. GAPDH was used to confirm that loading of lysates was equal. **Top Right:** Cells were treated with the indicated drugs for 24 hours and FACS analysis was performed to determine the amount of apoptosis (N = 3). Error bars representing standard deviation are shown by a line through each bar, and the percent of apoptosis can be seen on top of each bar. **Bottom Right:** Crystal violet assays were performed for combinational treatments. Cells were seeded in triplicates in a 96-well plate and the assays were performed 72 hours after treatment.

5.3 Ad-NOXA-induced cell death in HN8 is apoptosis

Due to the data suggesting that HN8 has a certain amount of cell death with NOXA induction alone, this cell line was used to explore both aims of this project. This section provides the results that address the mechanisms of Ad-NOXA in HN8 for the first part of **Aim 1**. First, the type of cell death induced by NOXA was analyzed to be apoptosis by using Q-VD-OPH (Quinoline-Val-Asp-Difluorophenoxymethyl Ketone), an irreversible inhibitor of caspase-1, caspase-3, caspase-8, and caspase-9 [www.enzolifesciences.com]. FACS analysis showed that when HN8 was treated with Ad-NOXA alone, cell death occurred to a significant amount (Figure 14). Ad-NOXA-induced cell death is mainly apoptosis because when Q-VD-OPH was added, cell death was dramatically decreased.

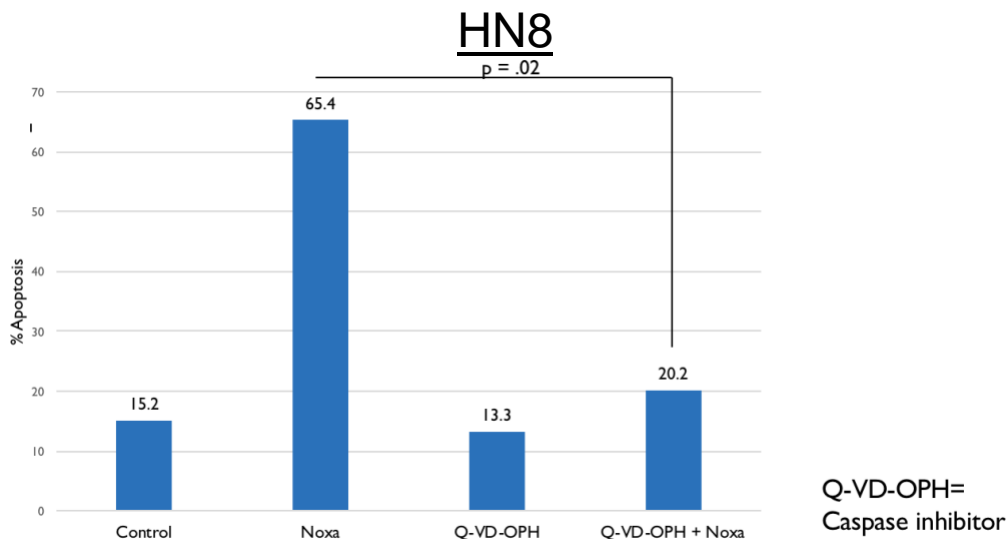


Figure 14: Ad-NOXA alone induces apoptosis in HN8. Cells were seeded in a 12-well plate and treated in duplicates with Control adenovirus (Ad-Con), Ad-NOXA, Q-VD-OPH with Ad-Con, and Q-VD-OPH with Ad-NOXA. The cells were trypsinized after 24 hours and analyzed using

FACS to determine the amount of apoptosis. The percent of apoptosis can be seen on top of each bar.

5.4 BAK contributes to NOXA-induced apoptosis

Now it is confirmed that NOXA-induced cell death is mainly apoptosis, the next step was to examine which BCL-2 family members contribute to NOXA-induced apoptosis to further address **Aim 1**. Short-hairpin RNA (shRNA) for BAK, BAX, or BIM were introduced in HN8 by lentiviruses. Each cell line was treated with Ad-Con or Ad-NOXA. Figure 15 shows that shBAK, shBAX, and shBIM stable cell lines were established and the expression of each protein was not altered by Ad-NOXA. For the control (shC), non-targeting shRNA was introduced.

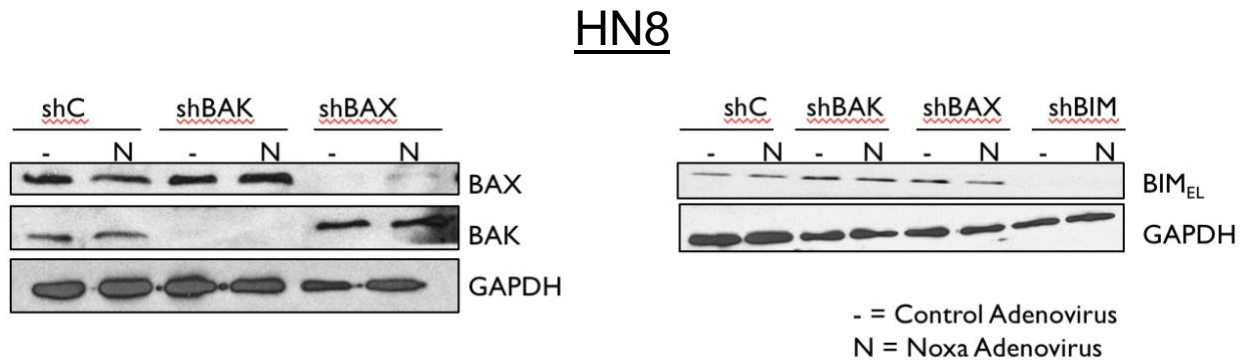


Figure 15: HN8 established shRNA knockdown cell lines for BAK (shBAK), BAX (shBAX), and BIM (shBIM). Lentiviruses encoding short-hairpin BAK, (shBAK), BAX (shBAX), BIM (shBIM), and scrambled control (shC) were infected in HN8 cells and stable cell lines were established with puromycin selection. The cells were then treated with Ad-Con and Ad-NOXA for 16 hours followed by Western blotting. GAPDH was used to show equal loading of cell lysates.

Once stable knockdowns were established for proteins of interest, FACS analysis was performed to see if BAK, BAX, or BIM contributed to cell death (Figure 16). The knockdown cell lines for BAK, BAX, and BIM were treated with Ad-Con and Ad-NOXA for 24 hours followed by FACS. The FACS analysis clearly shows a significant difference between HN8 shBAK treated with Ad-NOXA from HN8 shC with Ad-NOXA. There was no such difference in shBAX and shBIM cell lines, indicating that BAK contributes to NOXA-induced cell death in HN8 cells.

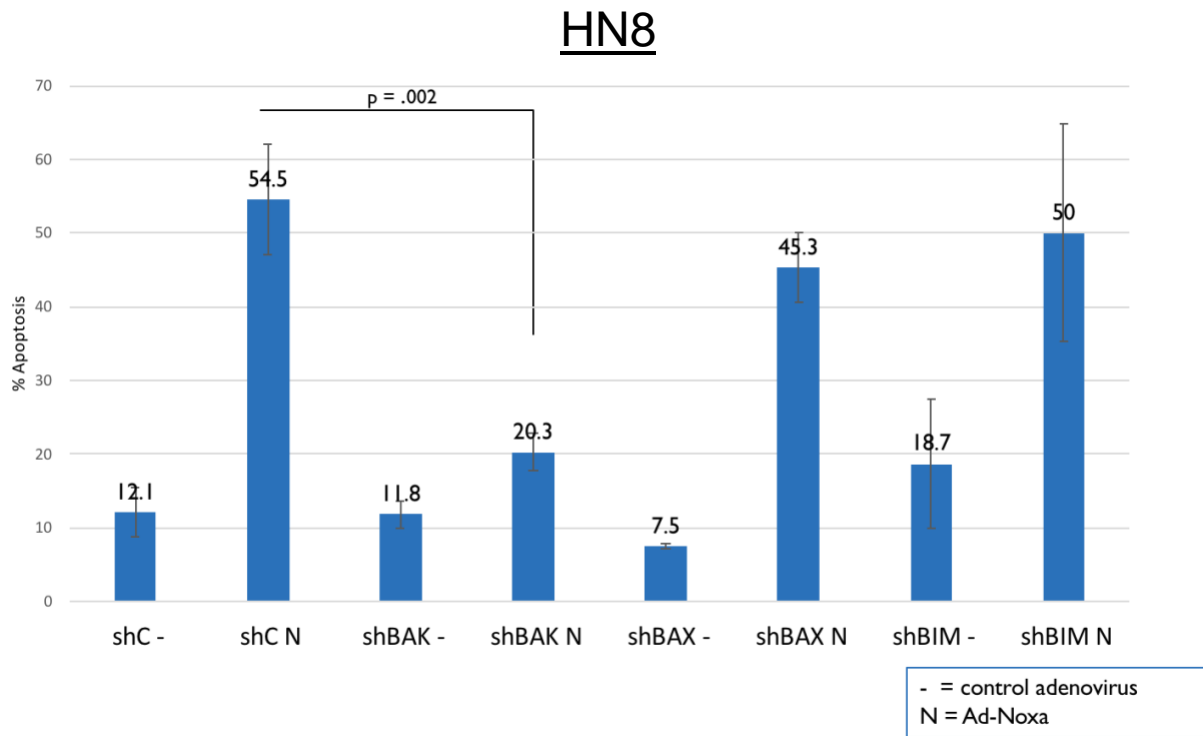


Figure 16: BAK is contributing to cell death. The cells in Figure 15 were treated with Ad-Con and Ad-NOXA for 24 hours followed by FACS to determine total amount of apoptosis (N = 3). Error bars representing standard deviation are shown by a line through each bar, and percentage of apoptosis for each cell line treatment is seen above each bar.

5.5 The mechanism of NOXA-induced cell death

Because the above results suggest that BAK is contributing to NOXA-induced apoptosis, the interactions of BIM, BAK, MCL-1, and NOXA were studied through immunoprecipitation experiments to further examine the mechanism for **Aim 1** (Figure 17). The input is HN8 cells treated with Ad-Con and Ad-NOXA for 16 hours. This is used as a control and is consistent with previous Western blot in Figure 13, showing that apoptosis is induced with Ad-NOXA alone because cleaved PARP is present. Additionally, NOXA is shown to be induced with Ad-NOXA.

The MCL-1 immunoprecipitation has interesting results (Figure 17, Left). Immunoprecipitated MCL-1 is seen to interact with BAK and BIM before NOXA induction. It is known that NOXA selectively binds to MCL-1^[34], and a strong binding of NOXA to immunoprecipitated MCL-1 can be seen in the Western blot (Figure 17, Left). After induction of NOXA, it binds to MCL-1, causing its inactivation. Then, BIM-MCL-1 and BAK-MCL-1 complexes are dissociated, which is suggested by the Western blot (Figure 17, Left). Next, the conformation change of BAK was examined by using a conformation-specific antibody to precipitate activated BAK. The Western blot shows a clear difference in band intensity for this specific BAK after NOXA is induced, indicating that a conformational change occurred (Figure 17, Right). The model for this data can be seen in Figure 18.

HN8

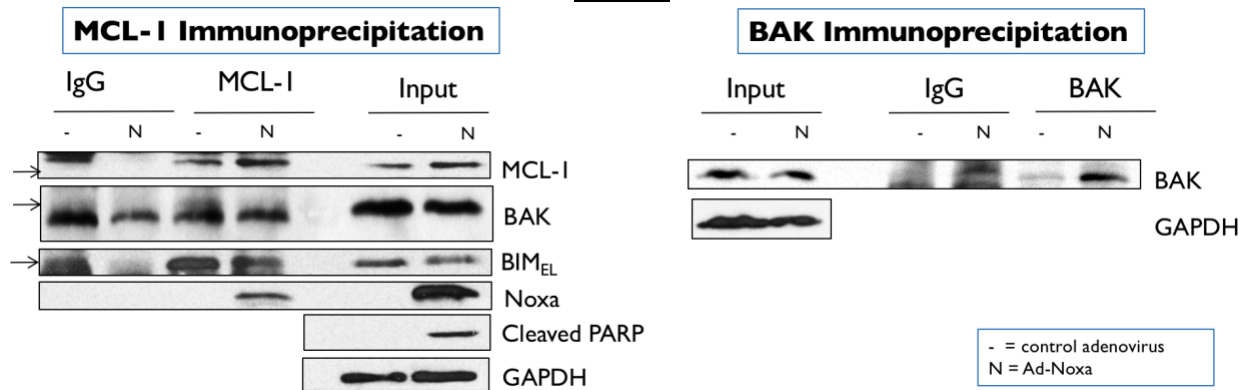


Figure 17: HN8 Immunoprecipitation experiments show BCL-2 family member interactions. HN8 cells (4×10^6) were seeded in a 10 cm dish in 10 mL of medium and treated with Ad-Con and Ad-NOXA the following day. After 16 hours, cells were harvested and equal amounts of protein were incubated with IgG, MCL-1 (Left), or conformation-specific BAK (Right) antibodies. The input represents 40/500 of the immunoprecipitated lysates. **Left:** Immunoprecipitation with MCL-1. **Right:** Immunoprecipitation with BAK that has undergone a conformational change. GAPDH was used to show equal loading of cell lysates.

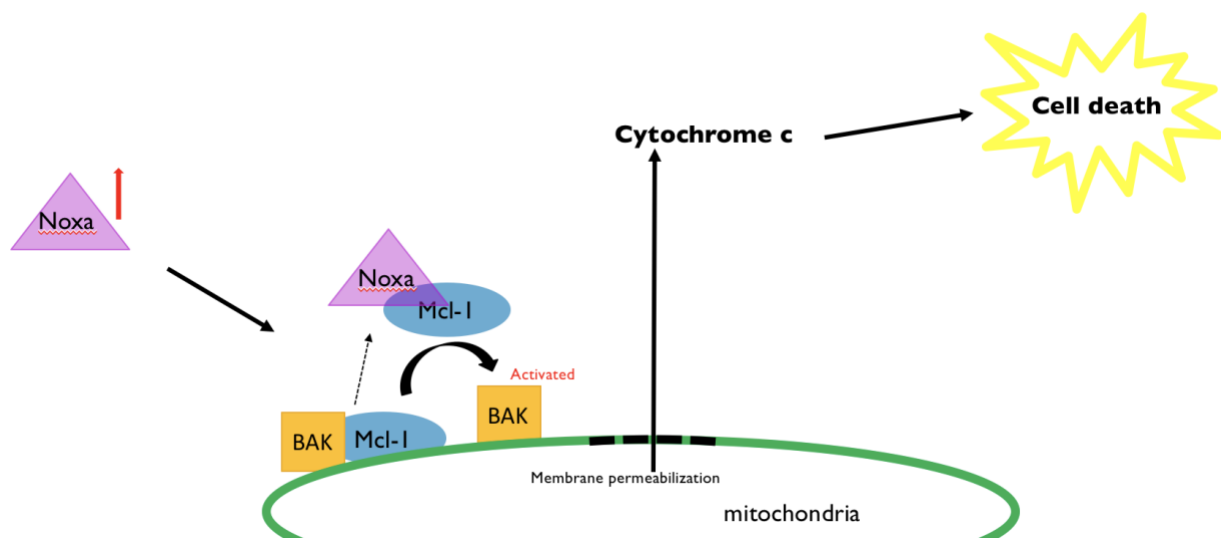


Figure 18: The mechanism of cell death induced by NOXA. When NOXA is induced, it sequesters MCL-1 from BAK. Then, BAK changes conformation, becomes activated, and oligomerizes on the mitochondrial membrane. MOMP occurs followed by cytochrome *c* release from the IMS into the cytosol and apoptosis occurs.

5.6 Fenretinide alone can induce cell death in HN8

Next, HN8 response to fenretinide was studied because fenretinide alone can efficiently induce apoptosis in HN8. This was done for the purpose of studying the mechanism of fenretinide-induced cell death in **Aim 2**. Both Western blot and FACS analysis show that NOXA is induced by fenretinide alone and in combination with ABT-263 (Figure 19). When the lentivirus encoding short-hairpin NOXA (shNoxa) is infected in HN8 cells, a clear decrease in the intensity of cleaved PARP can be seen as compared to HN8 shC with Western blot for fenretinide treatment. Similarly, there is a difference in intensity of cleaved PARP for combinational treatment of fenretinide with ABT-263 for HN8 shNOXA versus HN8 shC (Figure 19). This suggests that NOXA is contributing to cell death when HN8 is treated with fenretinide alone and in combination with ABT-263. FACS analysis is consistent with the

Western blot, showing more cell death comes from fenretinide and ABT-263 combination than fenretinide alone. Additionally, cell death comparison between combinational treatment in HN8 shC and shNOXA is significant, suggesting NOXA is important for fenretinide-induced cell death.

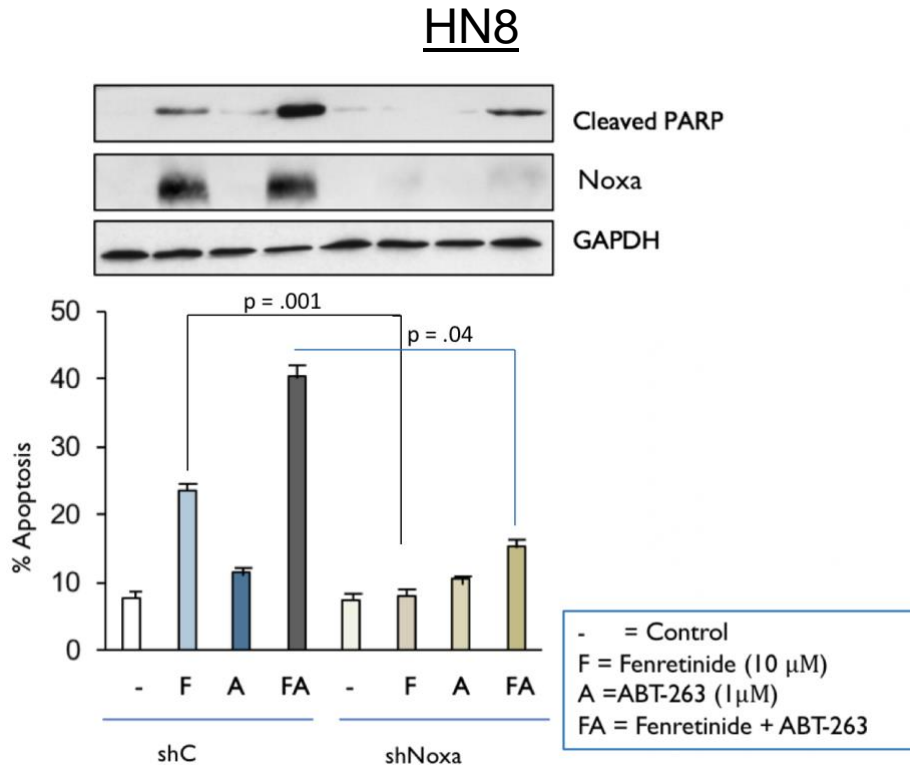


Figure 19: NOXA is contributing to Fenretinide-induced cell death. Lentiviruses encoding short-hairpin NOXA, (shNoxa) and scrambled control (shC) were infected in HN8 cells. **Top:** shC and shNoxa cells were treated with indicated drugs and harvested after 16 hours followed by Western blotting. Cells were probed with Cleaved PARP, NOXA, and GAPDH. GAPDH was used to show equal loading of cell lysates. **Bottom:** HN8 shC and shNOXA cells were treated with indicated drugs and trypsinized after 24 hours followed by FACS analysis. Error bars representing standard deviation are shown by a line through each bar.

5.7 Ad-NOXA or Fenretinide combined with ABT-263 show synergistic effects in HN12

HN8 can experience cell death with Ad-NOXA and fenretinide treatment alone. However, single treatment did not induce cell death in HN12, UMSCC1, or UMSCC47. These three cell lines were used to examine the mechanisms of combinational treatment as stated in **Aim 1** and **Aim 2**. To examine the reaction of HN12 to drug treatment by Western blot, cells were seeded in a 6-well plate and treated with Ad-NOXA, fenretinide (10 μ M), ABT-263 (1 μ M), or combinations (Figure 20, Left). The control was treated with Ad-Con. The cells were harvested overnight and the lysates were probed with cleaved PARP, MCL-1, BIM, NOXA, and GAPDH.

Similar analysis was done using FACS to confirm cell death amount that was qualitatively assessed by Western blotting. For FACS, HN12 cells were seeded in a 12-well plate and treated in duplicates with Ad-Con, Ad-NOXA, fenretinide (10 μ M), ABT-263 (1 μ M), or combinations (Figure 20, Top Right). After 24 hours, cells were trypsinized and FACS analysis was conducted.

Combinational treatments of Ad-NOXA or fenretinide with ABT-263 appears to have synergistic effects in HN12, as compared to single treatment. This is consistent in both Western blot through the amount of cleaved PARP and FACS analysis through the amount of apoptosis (Figure 20). Additionally, the Western blot shows that Ad-NOXA induces NOXA, but fenretinide alone and combined with ABT-263 do not induce NOXA.

To confirm that combinational treatment completely kills HN12 cells, crystal violet assays were done (Figure 20, Bottom Right). The crystal violet staining shows that cells have completely died with combinational treatment by the 72-hour point.

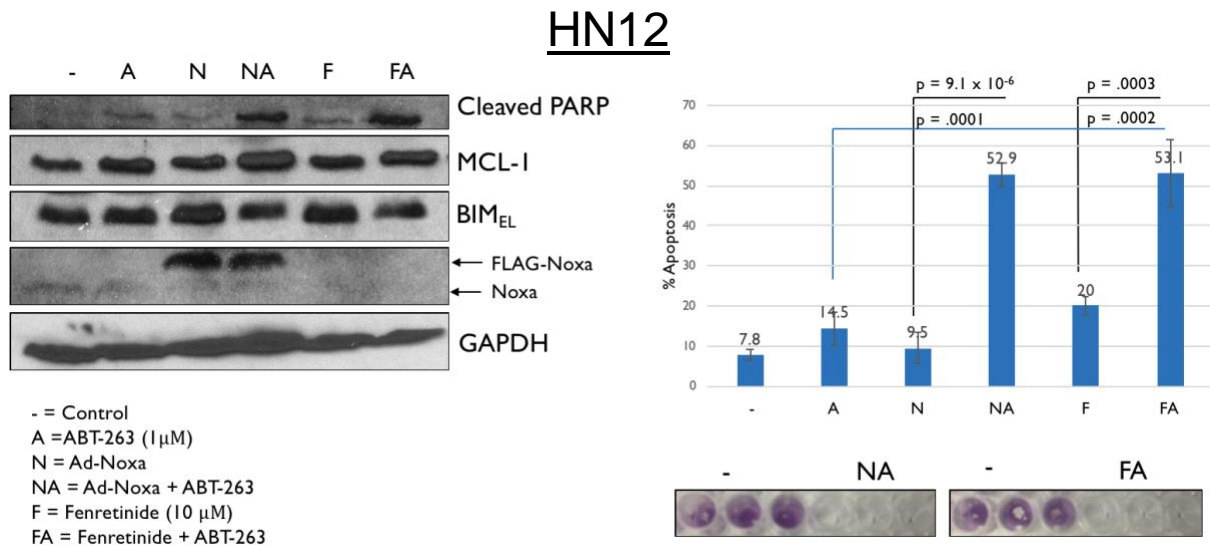


Figure 20: Ad-NOXA or Fenretinide in combination with ABT-263 has synergistic effects in HN12. **Left:** Cells were treated with indicated drugs for 16 hours, and samples were analyzed by Western blots with cleaved PARP, MCL-1, BIM, NOXA, and GAPDH. GAPDH was used to confirm that loading of lysates was equal. **Top Right:** Cells were treated with the indicated drugs for 24 hours, and FACS analysis was performed to determine the amount of apoptosis (N = 5). Error bars representing standard deviation are shown by a line through each bar, and the percent of apoptosis can be seen on top of each bar. **Bottom Right:** Crystal violet assays were performed for combinational treatments. Cells were seeded in triplicates in a 96-well plate, and the assays were performed 72 hours after treatment.

Combination of ABT-263 and Ad-NOXA showed synergistic effects in HN12, resulting in cell death. Ad-NOXA with ABT-263-induced cell death is mainly apoptosis because cell death was dramatically decreased when Q-VD-OPH was added with Ad-NOXA and ABT-263 (Figure 21).

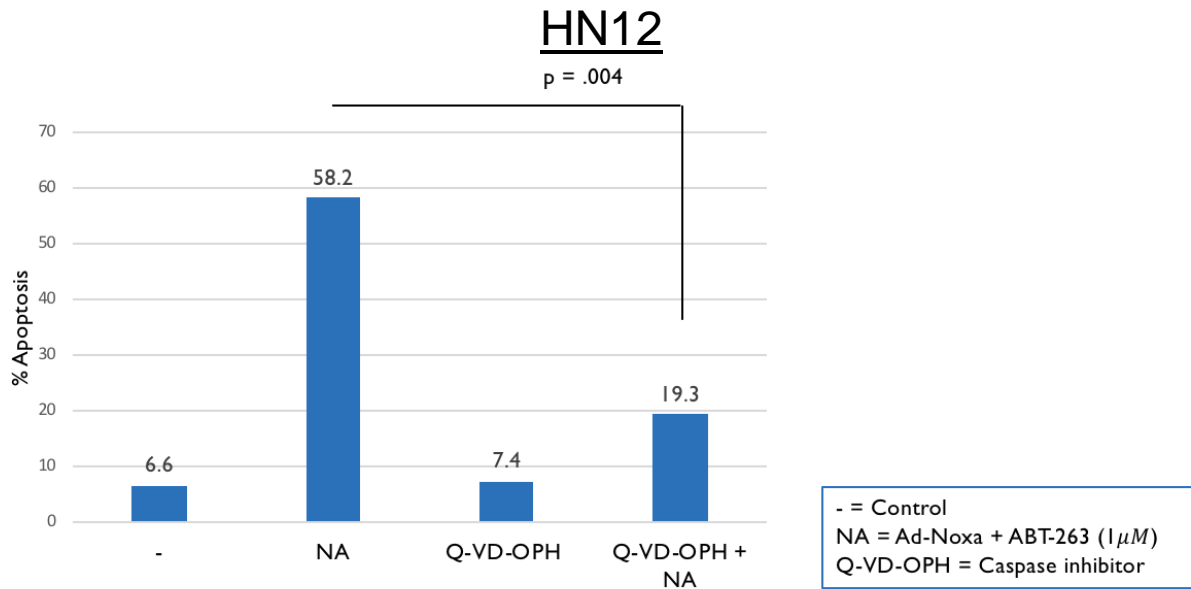


Figure 21: Combinational treatment of HN12 induces apoptosis. Cells were treated with Ad-Con, Ad-NOXA and ABT-263, Ad-Con with Q-VD-OPH, or Ad-NOXA and ABT-263 with Q-VD-OPH. The cells were trypsinized after 24 hours and analyzed using FACS to determine the amount of apoptosis. The percent of apoptosis can be seen on top of each bar.

5.8 The role of BIM in Ad-NOXA and ABT-263 combination-induced cell death in HN12

Next, an immunoprecipitation experiment was done in HN12 cells to examine the mechanism of combinational treatment of Ad-NOXA with ABT-263, which addresses the second part of **Aim 1**. HN12 cells were treated with ABT-263, Ad-NOXA, or a combination (Figure 22). Ad-Con was used as a control. BIM is clearly decreased when treated with ABT-263 or Ad-NOXA with ABT-263 (Figure 22). The immunoprecipitation with MCL-1 shows that the MCL-1 and BIM interaction appears significantly decreased with combinational treatment, suggesting BIM may be contributing to the combinational cell death (Figure 22).

The next step was to infect lentiviruses encoding short-hairpin BIM (shBIM) or scrambled control (shC) in HN12 cells to examine the role of BIM in cell death of HN12. Figure 23 confirms the knockdown of BIM. However, upon further examination using FACS analysis, there was no clear difference in cell death between HN12 shC and HN12 shBIM when cells were treated with Ad-NOXA, fenretinide, ABT-263, or combinations (Figure 23). This suggests that BIM does not play a role in combinational cell death in HN12.

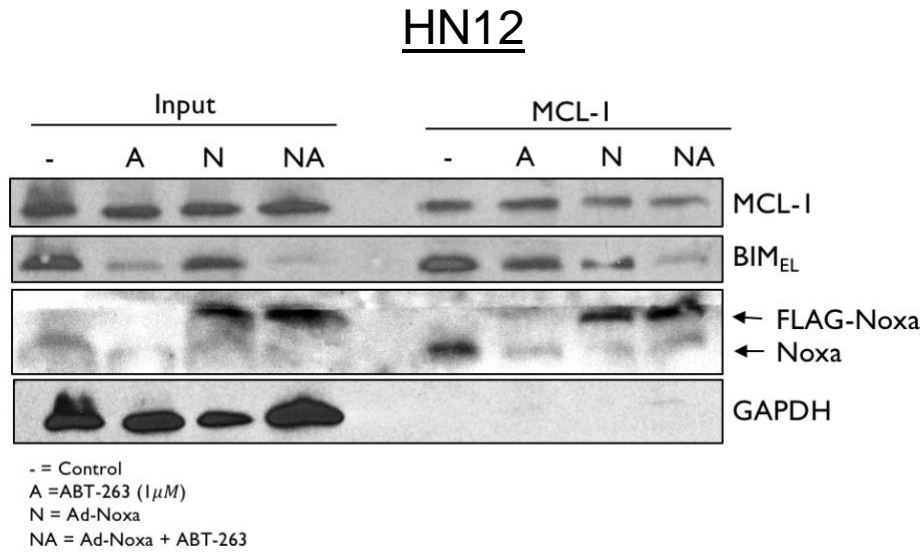


Figure 22: HN12 Immunoprecipitation with MCL-1. HN12 cells (4×10^6) were seeded in a 10 cm dish in 10 mL of medium and treated the following day with Ad-Con, ABT-263, Ad-NOXA, or a combination of Ad-NOXA and ABT-263. After 16 hours, cells were harvested and equal amounts of protein were incubated with MCL-1. The input represents 40/500 of the immunoprecipitated lysates.

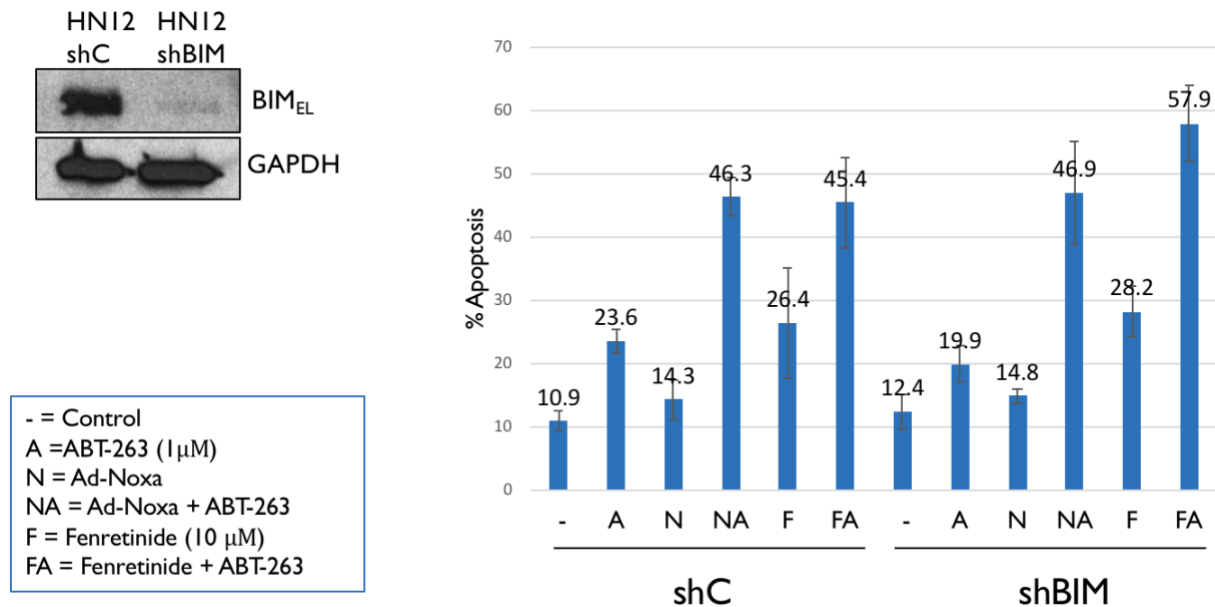


Figure 23: HN12 BIM knockdown data. **Left:** Lentiviruses encoding short-hairpin BIM (shBIM) or scrambled control (shC) were infected in HN12 cells and stable knockdown cells were established with puromycin selection. Western blotting was performed, and the membrane was probed with BIM and GAPDH antibodies. **Right:** Cells were treated with the indicated drugs for 24 hours and FACS analysis was performed to determine the amount of apoptosis (N = 3). Error bars representing standard deviation are shown by a line through each bar, and the percent of apoptosis can be seen on top of each bar.

5.9 Ad-NOXA or Fenretinide combined with ABT-263 shows increased cell death in other HNSCC cell lines

UMSCC1 and UMSCC47 were similar to HN12 in that single treatment did not induce efficient cell death. Both aims were addressed in these cell lines to examine cell death with drug treatment. To examine the reaction of UMSCC1 and UMSCC47 to drug treatment by Western blot, cells were seeded in a 6-well plate and treated with Ad-NOXA, fenretinide (10 μM), ABT-

263 (1 μM), or combinations (Figures 24 and 25). The control was treated with Ad-Con. The cells were harvested overnight and the lysates were probed with cleaved PARP, MCL-1, BIM, NOXA, and GAPDH.

Similar analysis was done using FACS to confirm cell death amount that was qualitatively assessed in the Western blot. For FACS, UMSCC1 and UMSCC47 cells were seeded in a 12-well plate and treated in duplicates with Ad-Con, Ad-NOXA, fenretinide (10 μM), ABT-263 (1 μM), or combinations (Figures 24 and 25). After 24 hours, cells were trypsinized and FACS analysis was performed.

UMSCC1 does not have much cell death when singly treated with Ad-NOXA or fenretinide, which can be seen from cleaved PARP in the Western blot, as well as the percentage of apoptosis from FACS analysis (Figure 24). Additionally, the combination of Ad-NOXA with ABT-263 suggests a synergizing relationship, leading to apoptosis. The combination of fenretinide with ABT-263, on the other hand, does seem to increase cell death, but only with an additive effect. To confirm that combinational treatment completely kills UMSCC1 cells, crystal violet assays were done (Figure 24, Bottom Right). The crystal violet staining shows that cells have completely died with combinational treatment by the 72-hour point.

UMSCC1

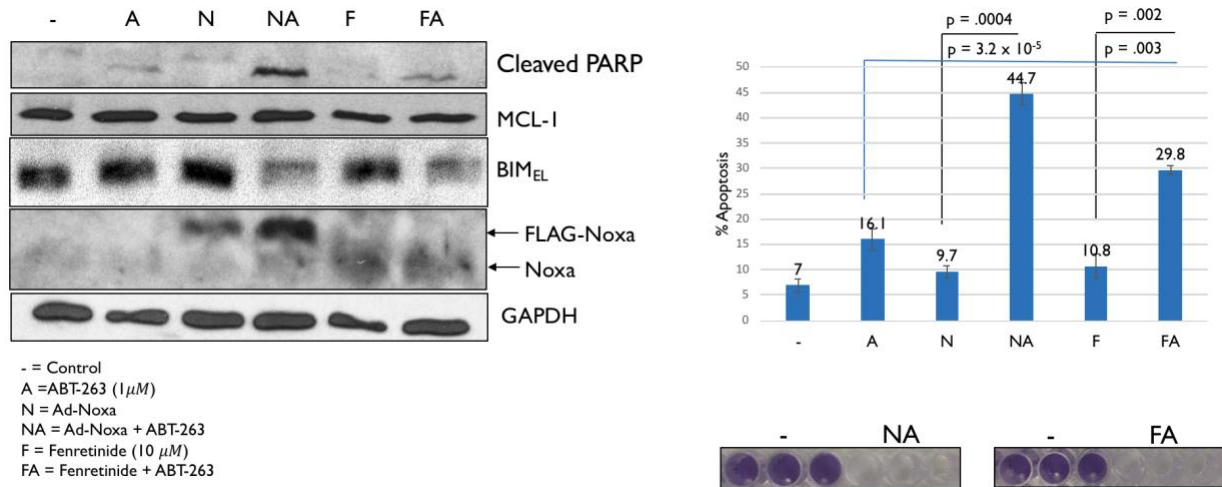


Figure 24: Ad-NOXA or Fenretinide in combination with ABT-263 increases cell death in UMSCC1. **Left:** Cells were treated with indicated drugs for 16 hours, and samples were analyzed by Western blot with cleaved PARP, MCL-1, BIM, NOXA, and GAPDH. GAPDH was used to confirm that loading of lysates was equal. **Top Right:** Cells were treated with the indicated drugs for 24 hours and FACS analysis was performed to determine the amount of apoptosis (N = 3). Error bars representing standard deviation are shown by a line through each bar, and the percent of apoptosis can be seen on top of each bar. **Bottom Right:** Crystal violet assays were performed for combinational treatments. Cells were seeded in triplicates in a 96-well plate, and the assays were performed 72 hours after treatment.

Western blot and FACS analysis suggest that UMSCC47 does not have much cell death when singly treated with Ad-NOXA or fenretinide (Figure 25). In contrast, combinational treatments of both Ad-NOXA and fenretinide with ABT-263 seem to have a synergistic effect.

Similar to HN8 and HN12, NOXA is induced with Ad-NOXA and its combination with ABT-263 in UMSCC1 and UMSCC47 (Figure 24, Left and Figure 25, Left). Additionally, UMSCC1 and UMSCC47 both have NOXA induction with fenretinide treatment, as well as its

combination with ABT-263, providing the results for **Aim 2**. This was the case for HN8, as can be seen from the Western blot (Figure 13, Left). However, HN12 did not show a detectable signal for NOXA with fenretinide or fenretinide with ABT-263 treatment (Figure 20, Left).

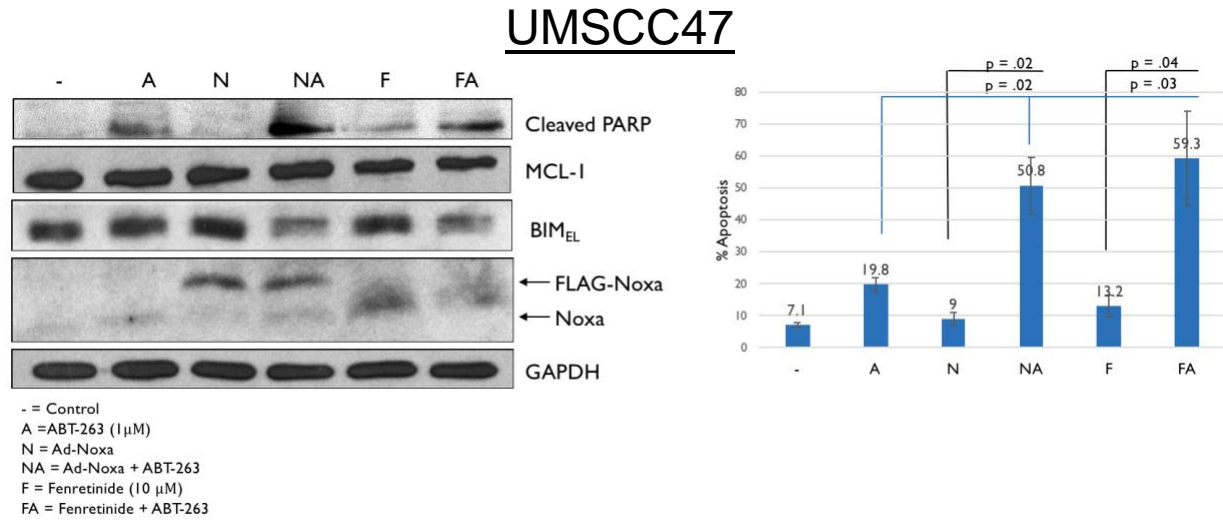


Figure 25: Ad-NOXA or Fenretinide in combination with ABT-263 has a synergistic effect in UMSCC47. Left: Cells were treated with indicated drugs for 16 hours, and samples were analyzed by Western blots with cleaved PARP, MCL-1, BIM, NOXA, and GAPDH. GAPDH was used to confirm that loading of lysates was equal. **Right:** Cells were treated with the indicated drugs for 24 hours, and FACS analysis was performed to determine the amount of apoptosis (N = 3). Error bars representing standard deviation are shown by a line through each bar, and the percent of apoptosis can be seen on top of each bar.

5.10 Mouse head and neck cancer cell lines and protein expression

In addition to the four human cell lines studied, analysis was also done on five HNSCC mouse cell lines. The mouse cell lines were established with a 4NQO mouse model, causing mice to form spontaneous tumors on their tongues (refer to section 4.1).

Figure 26 shows a Western blot of all five mouse cell lines with expression of p53 and BCL-2 family members. It appears that p53 and BIM status vary in these cell lines. However, the other BCL-2 family members show relatively equal levels (Figure 26, Left). A Western blot of the mouse cell lines with a non-cancerous tongue specimen is also seen to determine the normal levels of protein in a mouse for comparison (Figure 26, Right). This Western blot shows that p53 for 601 and 606 appears to be in a different position compared to the normal mouse. Also, 606 shows a much stronger intensity than any other cell lines or the normal mouse. Additionally, it seems that the level of p53 is undetectable in 613. This variation is similar to human HNSCC because p53 alterations occur in over half of cancer cases^[60]. Additionally, the BIM level appears to be elevated in 604 (Figure 26).

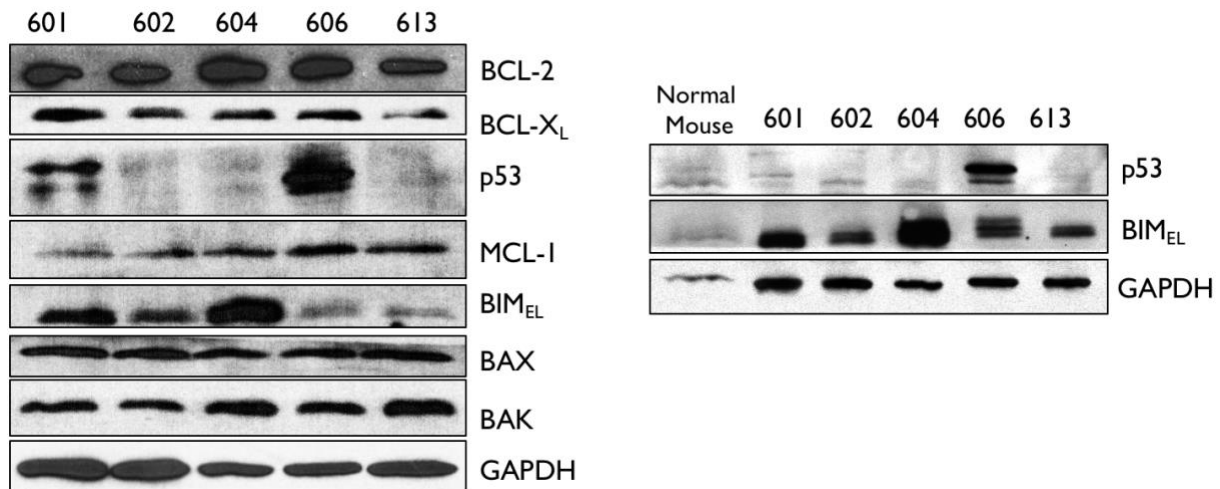


Figure 26: Western Blot of mouse cell lines. Left: The Western blot shows mouse cell lines indicated. Cells were seeded on the plates and harvested overnight. Samples were analyzed by Western blot with BCL-X_L, p53, MCL-1, BIM, BAX, and BAK. **Right:** The Western blot shows mouse cell lines indicated, as well as a normal mouse, non-cancerous specimen from the tongue. The samples were analyzed by Western blot with p53, BIM, and GAPDH. GAPDH was used to confirm that loading of lysates was equal.

5.11 Combinational treatment increases cell death in mouse HNSCC cells.

Mouse HNSCC cell lines were treated in a similar fashion to the human HNSCC cell lines to examine apoptosis. To examine the reaction of 601 and 606 to drug treatment by Western blot, cells were seeded in a 6 cm dish and treated with Ad-NOXA, fenretinide (10 μ M), ABT-263 (0.5 μ M), or combinations (Figures 27 and 28). The control was treated with Ad-Con. The cells were harvested overnight and the lysates were probed with cleaved PARP, MCL-1, BIM, NOXA, and GAPDH.

Similar analysis was done using FACS to confirm cell death amount that was qualitatively assessed in the Western blot. 601, 606, 602, and 613 cells were seeded in a 12-well plate and treated in duplicates with Ad-Con Ad-NOXA, fenretinide (10 μ M), ABT-263 (0.5 μ M), and combinations (Figures 27, 28, 29, and 30). After 24 hours, cells were trypsinized and FACS analysis was performed.

601, 606, 602, and 613 do not have much cell death when singly treated with Ad-NOXA or fenretinide, which can be seen from cleaved PARP in the Western blot, as well as the percentage of apoptosis from FACS analysis (Figures 27, 28, 29, and 30). Additionally, in 601, the combination of Ad-NOXA with ABT-263 appears to have a synergistic relationship. In 606, 602, and 613, the effect of this combination does increase cell death, but likely with an additive effect.

The combination of fenretinide with ABT-263, on the other hand, does not seem to increase cell death significantly in 613 (Figure 30). However, the combination of fenretinide with ABT-263 does increase cell death in 606 and 602 (Figure 28, Left and Figure 29). In 601, there is no significant difference for the combination of fenretinide and ABT-263 as compared to single treatments (Figure 27). However, there is a significant difference in the amount of

apoptosis between untreated cells and cells treated with the combination of fenretinide and ABT-263 (Figure 27). To confirm that combinational treatment kills 601 and 606 cells, crystal violet assays were done (Figure 27, Bottom Right and Figure 28, Bottom Right). The crystal violet staining shows that cells have died with combinational treatment by the 96-hour point.

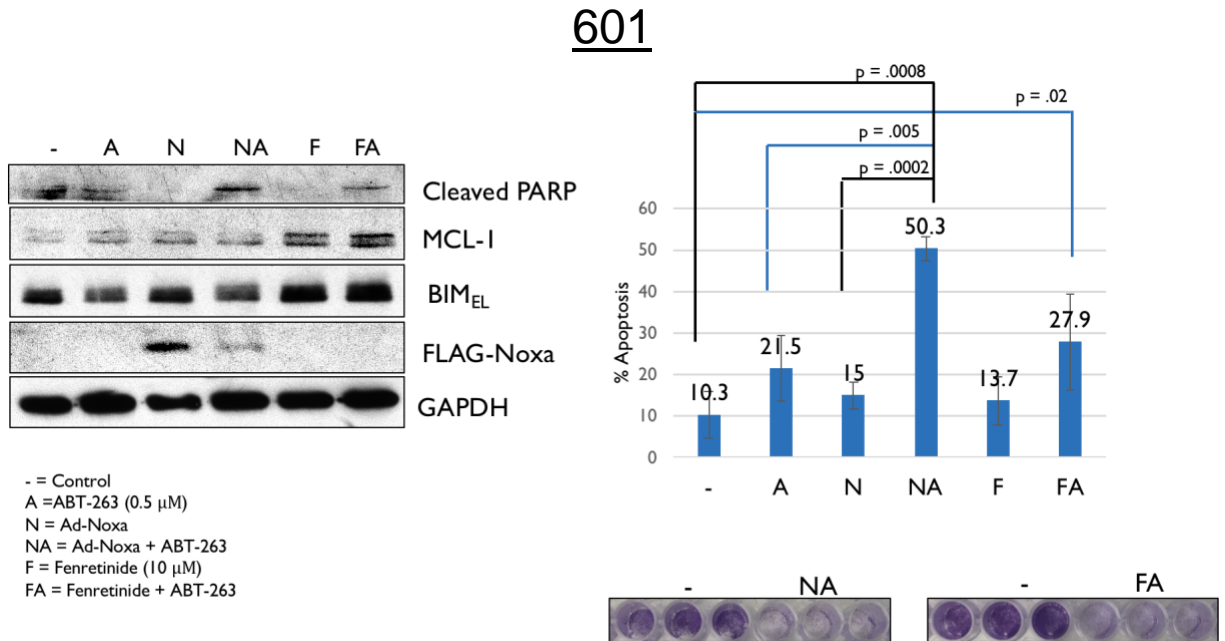


Figure 27: Ad-NOXA and ABT-263 combinational treatment has a synergistic effect in 601, but Fenretinide and ABT-263 treatment does not produce as much cell death. Left: Cells were treated with indicated drugs for 16 hours, and samples were analyzed by Western blot with cleaved PARP, MCL-1, BIM, NOXA, and GAPDH. GAPDH was used to confirm that loading of lysates was equal. **Top Right:** Cells were treated with the indicated drugs for 24 hours, and FACS analysis was performed to determine the amount of apoptosis (N = 4). Error bars representing standard deviation are shown by a line through each bar, and percent of apoptosis can be seen on top of each bar. **Bottom Right:** Crystal violet assays were performed for

combinational treatments. Cells were seeded in triplicates in a 96-well plate, and the assays were performed 72 hours after treatment.

606

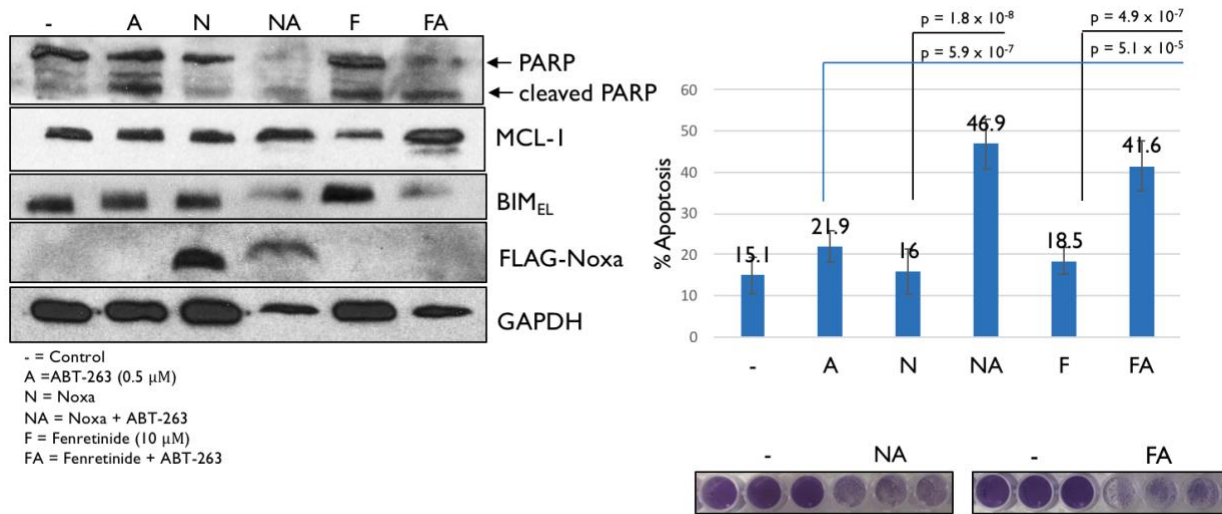


Figure 28: Ad-NOXA and Fenretinide in combination with ABT-263 increases cell death in 606. **Left:** Cells were treated with indicated drugs for 16 hours, and samples were analyzed by Western blots with total PARP, MCL-1, BIM, NOXA, and GAPDH. GAPDH was used to confirm that loading of lysates was equal. **Top Right:** Cells were treated with the indicated drugs for 24 hours, and FACS analysis was performed to determine the amount of apoptosis (N = 9). Error bars representing standard deviation are shown by a line through each bar, and the percent of apoptosis can be seen on top of each bar. **Bottom right:** Crystal violet assays were performed for combinational treatments. Cells were seeded in triplicates in a 96-well plate, and the assays were performed 96 hours after treatment.

602

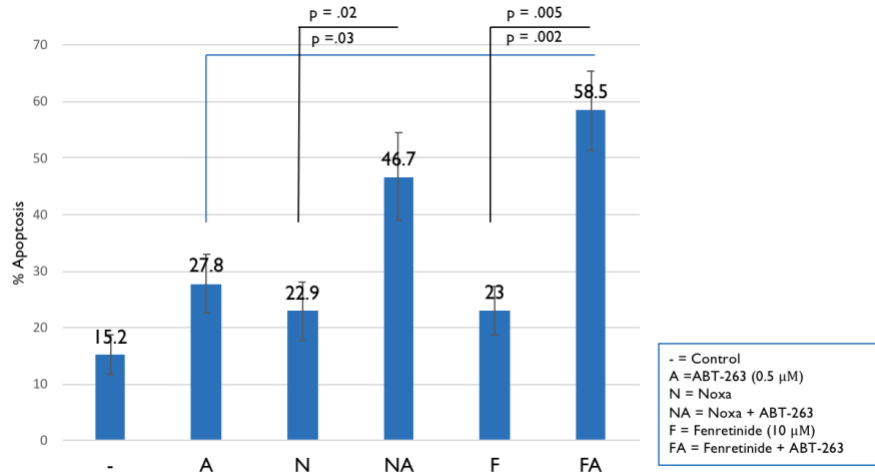


Figure 29: Ad-NOXA or Fenretinide with ABT-263 combinational treatment increases cell death in 602. Cells were treated with the indicated drugs for 24 hours, and FACS analysis was performed to determine the amount of apoptosis (N = 4). Error bars representing standard deviation are shown by a line through each bar, and the percent of apoptosis can be seen on top of each bar.

613

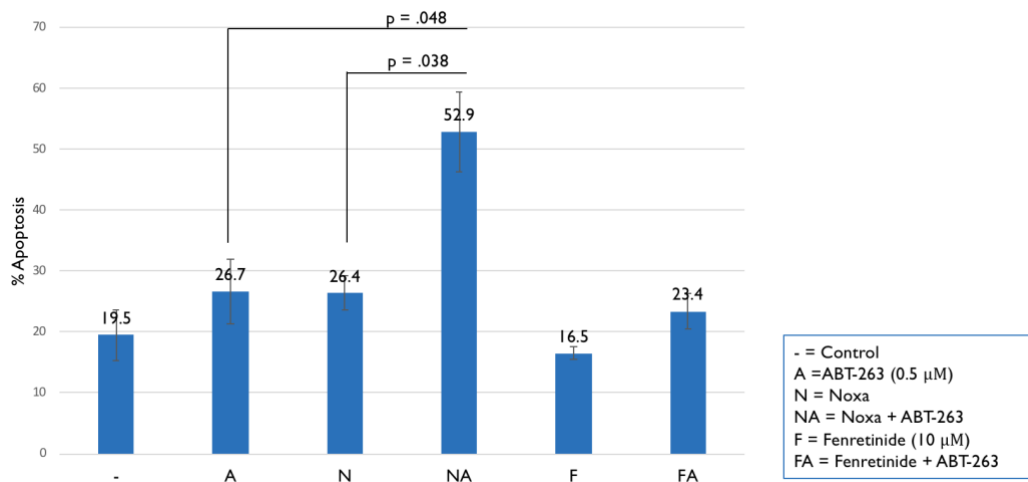


Figure 30: Ad-NOXA and ABT-263 combinational treatment increases cell death in 613, but Fenretinide and ABT-263 treatment does not produce as much cell death. Cells were treated

with the indicated drugs for 24 hours, and FACS analysis was performed to determine the amount of apoptosis (N = 3). Error bars representing standard deviation are shown by a line through each bar, and the percent of apoptosis can be seen on top of each bar.

Discussion

6.1 NOXA-induced cell death leads to BAK activation

In HN8, Ad-NOXA treatment alone induces apoptosis (Figure 14). This cell line is different from all other human cell lines examined in which single treatments did not induce significant amounts of cell death (Figures 20, 21, 24, and 25). Thus, the first focus became on NOXA-induced cell death to understand the mechanism, which is the first part of **Aim 1**.

To determine which BCL-2 family members were contributing, stable shRNA knockdowns were established for BAK, BAX, and BIM in HN8 (Figure 15). These BCL-2 family members were chosen because BIM is a direct activator of BAK and BAX, and BAK and BAX are downstream effector proteins^[16]. While only one construct was used for these shRNA knockdowns due to time constraints, future studies would confirm these results with other constructs.

FACS analysis with HN8 shBAK, shBAX, and shBIM suggested BAK mainly contributed to NOXA-induced cell death (Figure 16). This knockdown data is consistent with the model that when NOXA is induced, it sequesters MCL-1 from BAK, leading to the degradation of MCL-1 (Figure 18). From here, BAK goes through a conformational change, is activated, and homo-oligomerizes to form a pore in the OMM. Then, cytochrome *c* is released from the IMS into the cytosol, and apoptosis occurs.

To further confirm the mechanism for NOXA-induced apoptosis for **Aim 1**, immunoprecipitation experiments were done with antibodies for MCL-1 and for the activated form of BAK in HN8 (Figure 17). After NOXA induction, a reduced interaction between MCL-1 and BAK and activation of BAK was observed. Although the result from BAK/MCL-1 interaction is not strikingly clear, there is still a presence of a band of BAK for the MCL-1

immunoprecipitation before Ad-NOXA treatment, and this band is decreased after NOXA induction (Figure 17, Left). Additionally, activated BAK appears to have a significant increase after Ad-NOXA treatment, supporting the proposed mechanism (Figure 17, Right). It is also important to note that the BIM and MCL-1 interaction is decreased after NOXA treatment. While this is the case, results from the shRNA BIM knockdown suggest that BIM is not a major player in NOXA-induced cell death. It is likely that when NOXA is introduced, the interaction between BIM and MCL-1 is interrupted (Figure 17, Left). However, BIM could be sequestered by the other anti-apoptotic BCL-2 family members BCL-2 and BCL-X_L, explaining why BIM does not play a significant role in NOXA-induced cell death (Figure 16).

6.2 NOXA contributes to Fenretinide-induced cell death

While Ad-NOXA alone induces cell death in HN8, so does fenretinide alone. Thus, HN8 was used to study the mechanism of fenretinide alone for **Aim 2** (Figure 13). Lentivirus encoding shNOXA was introduced into HN8 cells to determine if NOXA contributed to fenretinide-induced cell death. The Western blot and FACS analysis showed that NOXA contributed to fenretinide-induced cell death and in combination with ABT-263 (Figure 19) because cleaved PARP is decreased in HN8 shNOXA for fenretinide treatment or fenretinide with ABT-263 treatment.

Future studies would include conducting FACS analysis with HN8 shC, shBAK, shBAX, and shBIM for fenretinide treatment to further examine this mechanism for **Aim 2**. The expectation would be similar to the results of Ad-NOXA, where BAK would contribute to fenretinide-induced cell death. Additionally, immunoprecipitation experiments with fenretinide need to be performed in future studies to confirm the interactions of BCL-2 family members. We

expect that fenretinide immunoprecipitations will have similar results as Ad-NOXA immunoprecipitations in HN8, UMSCC1, and UMSCC47, because fenretinide significantly induces NOXA.

6.3 Combinational treatment of ABT-263 with Ad-NOXA or Fenretinide enhanced cell death in HNSCC cells

HN8, HN12, UMSCC1, and UMSCC47 all exhibited an increase in apoptosis for combinational treatments of fenretinide and Ad-NOXA with ABT-263, as compared to single treatments. These findings support the hypothesis that combinational treatment of Ad-NOXA or Fenretinide with ABT-263 induces and increases cell death in HNSCC cells. However, all these cell lines had slightly different findings.

HN8 is different from other HNSCC cell lines because single treatment can efficiently induce apoptosis. Also, there is a significant increase in cell death when ABT-263 is added to Ad-NOXA or fenretinide. This increase appears to be additive for both combinations in HN8 (Figure 13).

HN12, UMSCC1, and UMSCC47 are not affected greatly by treatment of Ad-NOXA or fenretinide alone. In HN12, the Western blot and FACS data suggest that ABT-263 with Ad-NOXA or fenretinide have a synergistic effect (Figure 20). HN12 is also different from the other human cell lines because fenretinide does not induce NOXA, as can be seen from the Western blot (Figure 20, Left). Future studies would include determining which BCL-2 family members are important in ABT-263 and fenretinide-induced cell death for HN12.

While the mechanisms of cell death with the combination of fenretinide and ABT-263 seem to be different in HN12, results prove interesting for the mechanism of the combination of

Ad-NOXA and ABT-263. HN12 was used to study the second part of **Aim 1** for the mechanism of combinational treatment of Ad-NOXA with ABT-263. Immunoprecipitation data of HN12 suggested that BIM contributes to cell death because the BIM and MCL-1 interaction appears to be significantly decreased (Figure 22). However, upon further examination, there was no significant difference in amount of cell death examined between HN12 shBIM and HN12 shC when treated with Ad-Con, Ad-NOXA, ABT-263, or combinations, suggesting that BIM does not contribute significantly in cell death of HN12 with the treatments mentioned (Figure 23).

HN12 does not show efficient cell death with single treatments, but in HN8, NOXA alone can induce cell death by specifically binding to and inactivating MCL-1^[27]. It was found that BAK contributed mainly to NOXA-induced cell death, and the model proposed can be seen in Figure 18. In HN12, ABT-263 is needed in combination with Ad-NOXA to efficiently induce cell death. As mentioned in section 1.9, ABT-263 inactivates pro-survival proteins BCL-2 and BCL-XL. These pro-survival proteins can interact with and regulate both BAK and BAX. Thus, we speculate that both BAK and BAX contribute to cell death by Ad-NOXA and ABT-263 combination in HN12. To examine this hypothesis and successfully fulfill the second part of **Aim 1**, it is essential to establish shRNA knockdowns for BAK (shBAK) and BAX (shBAX) in HN12.

Unlike HN12, UMSCC1 and UMSCC47 show the induction of NOXA when treated with fenretinide or fenretinide in combination with ABT-263, which addresses the mechanism of these drug treatments in **Aim 2** (Figure 20, Left; Figure 24, Left; Figure 25, Left). Future studies would need to establish shRNA knockdown cell lines for NOXA to prove that NOXA is contributing to fenretinide and ABT-263 combination-induced cell death in both UMSCC1 and UMSCC47.

UMSCC1 also has increased cell death for ABT-263 in combination with Ad-NOXA and fenretinide (Figure 24). ABT-263 and Ad-NOXA combinational treatment seems to have a synergistic effect, while ABT-263 and fenretinide combination appears to have an additive effect. In addition, UMSCC47 had similar findings to the other human cell lines in terms of combinational treatments. In this cell line, combination of ABT-263 with Ad-NOXA or Fenretinide has a synergistic effect (Figure 25).

The mechanisms for cell death in combination of ABT-263 with Ad-NOXA or fenretinide still need to be examined further to fulfill parts of **Aim 1** and **Aim 2**. Future studies would include immunoprecipitation experiments of BCL-2 and BCL-XL with ABT-263 to confirm their reactions.

6.4 Combinational treatment of ABT-263 with Ad-NOXA or Fenretinide was independent of p53 status

It is important to note that the *p53* status varies in the four cell lines examined. Because *p53* is a tumor suppressor protein that is involved in cell cycle regulation and apoptosis, we wanted to see how each cell line responded to the drug treatments tested. Figure 12 shows the various *p53* status of the four HNSCC cell lines used in this study. While all four cell lines did not behave exactly the same, combinational treatment of ABT-263 with Ad-NOXA or fenretinide did increase cell death in HN8, HN12, UMSCC1, and UMSCC47 (Figures 13, 20, 24, and 25). With knowledge that chemotherapeutic drugs can induce NOXA in a *p53*-independent manner and the findings presented, the results strongly suggest that the combination treatments tested here are independent of *p53* status.

6.5 Mouse HNSCC cell lines are responsive to combinational treatment

Because *in vivo* mouse models will be studied in the future, mouse HNSCC cell lines were established from five different mice's primary tongue tumors. The cell lines were treated and analyzed by Western blot and FACS analysis. Each cell line established exhibited varying levels of proteins and different results with cell death analysis. This is similar to human patient populations because each individual is drastically different.

From the data collected, no mouse cell lines result in a significant amount of apoptosis with single treatments. However, combinational treatment of ABT-263 with Ad-NOXA increases cell death in 601, 606, 602, and 613 (Figures 27, 28, 29, and 30). This suggests that this combination is also working well in mouse HNSCC cells.

Out of the mouse cell lines examined, 606 and 602 show significantly increased cell death by fenretinide and ABT-263 combinational treatment compared to single treatments (Figures 28 and 29). It can be hypothesized that 606 and 602 are responding well to these treatments because fenretinide induces NOXA efficiently. Since there are no appropriate antibodies for mouse NOXA, this can be studied in the future by for **Aim 2** by quantifying mRNA by Q-PCR to determine NOXA mRNA levels.

In addition, the Western blot of mouse cells shows that the intensity and position of the band for p53 in 606 is different from the normal mouse (Figure 26). The intensity is drastically stronger than any other cell lines or the normal mouse, and we can speculate that the p53 status of 606 may be the reason this cell line is more susceptible to apoptosis.

The position of p53 in 601 also appears to be different from the normal mouse (Figure 26). In addition, the signal of p53 in 613 is clearly less than the normal mouse. While 601, 606, and 613 all may have different p53 status than the normal mouse, the Western blot shows that

p53 for 602 and 604 is in the same position as the normal mouse, suggesting that all three have the same p53 status. However, the Western blot also shows that much less of the normal mouse lysate was loaded into the SDS-polyacrylamide gel. We can speculate many things about 602 and 604 from these observations. Perhaps one allele of *p53* is deleted, while the other is wild-type (WT).

Similar to the p53 status, the BIM expression varies amongst the cell lines with 604 showing the strongest signal from the Western blot (Figure 26). To clarify the status of BIM, p53, and other proteins and to further examine speculations mentioned, it is essential to study the DNA, RNA, and protein stability of these cell lines. It is known, for example, that stability of p53, MCL-1, and BIM are all affected by phosphorylation status^[41, 57, 61]. Many proteins are regulated at transcriptional, post-transcriptional, and post-translational levels. Understanding the DNA, RNA, and protein stability would provide evidence behind the changed protein status in these cell lines, as well as provide some evidence for hypotheses made.

In conclusion, all mouse HNSCC cell lines are different, which can be concluded from the Western blot showing varying levels of proteins, as well as varying effects of treatment when treated with the Ad-Con, ABT-263, Ad-NOXA, fenretinide or combinations. Like human tumors, these mouse tumors are multifaceted, and it is our goal to determine a common treatment method with identification of biomarkers that can successfully kill cancer cells.

Conclusion

The data presented show an increase in apoptosis for combinational treatments of fenretinide or Ad-NOXA with ABT-263, as compared to single treatments. Pro-survival MCL-1 is inhibited by NOXA, while pro-survival BCL-2 and BCL-X_L are inactivated by ABT-263 simultaneously,

contributing to an increase in cell death (Figure 31). In conclusion, combinational treatment of Ad-NOXA or Fenretinide with ABT-263 induces and increases cell death by simultaneously inhibiting all anti-apoptotic BCL-2 family proteins in HNSCC cells.

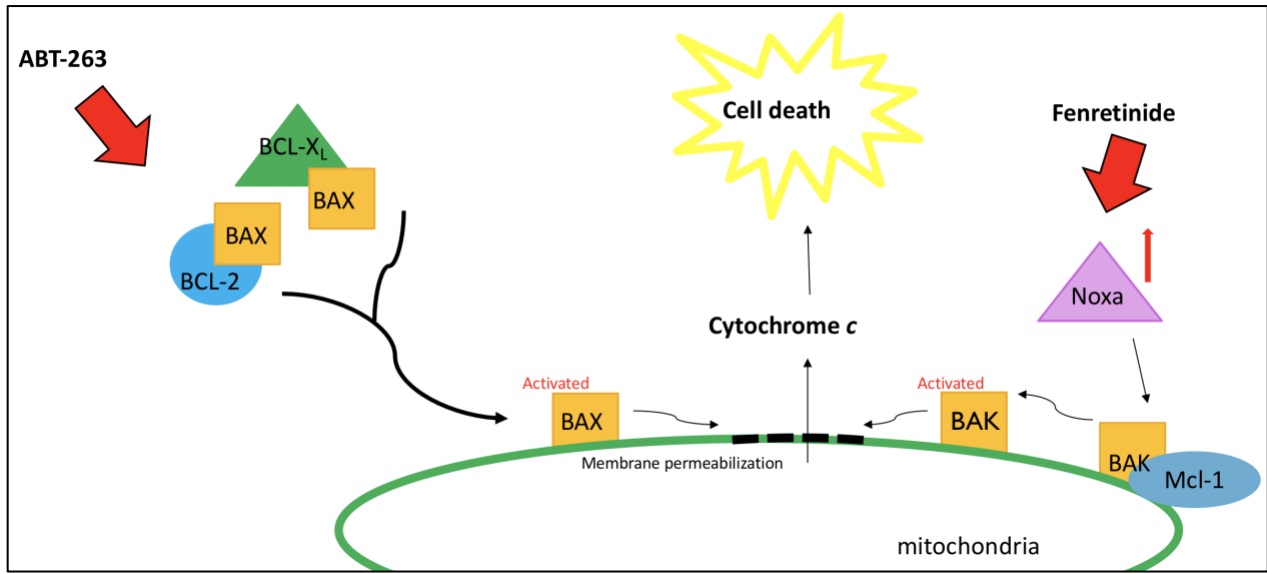


Figure 31: The mechanism of cell death induced by combinational treatment. When NOXA is induced, it sequesters and inactivates MCL-1. When ABT-263 is introduced into the cell, it inactivates BCL-2 and BCL-XL. The combination of NOXA induction and ABT-263 treatment inactivate all anti-apoptotic proteins, causing BAK and BAX activation and apoptosis.

Literature Cited

1. Siegel, R.L., Miller, K.D., & Jemal, A. (2018). Cancer statistics, 2018. *CA: A Cancer Journal for Clinicians*, 68 (1): 7-30.
2. Sanderson, R. J., & Ironside, J. A. D. (2002). Squamous cell carcinomas of the head and neck. *BMJ: British Medical Journal*, 325(7368), 822–827.
3. American Cancer Society (2018). Cancer Facts and Figures 2018. Atlanta, GA: American Cancer Society. Retrieved March 1, 2018.
4. Blot WJ, McLaughlin JK, Winn DM, et al. (1988) Smoking and drinking in relation to oral and pharyngeal cancer. *Cancer Research* 1988; 48(11):3282–3287
5. Hashibe M, Brennan P, Benhamou S, et al. (2007). Alcohol drinking in never users of tobacco, cigarette smoking in never drinkers, and the risk of head and neck cancer: pooled analysis in the International Head and Neck Cancer Epidemiology Consortium. *Journal of the National Cancer Institute*; 99(10):777–789.
6. Gillison ML, D’Souza G, Westra W, et al. (2008). Distinct risk factors profiles for human papillomavirus type 16-positive and human papillomavirus type-16 negative head and neck cancers. *Journal of the National Cancer Institute* ; 100(6):407–420.
7. Edge, SB. (2010). AJCC Cancer Staging Manual. *AJCC Cancer Staging Manual*. (pp. 21-100). New York, New York: Springer
8. Ward, D. E. C., & van, A. C. J. (2014). *Head and Neck Cancer: Treatment, Rehabilitation, and Outcomes*. Retrieved from <https://ebookcentral-proquest-com.proxy.library.vcu.edu>
9. Heron, D., Tishler, R., & Thomas, C. (Eds.). (2011). *Head and neck cancer*. (pp. 183-1200). Retrieved from <https://ebookcentral-proquest-com.proxy.library.vcu.edu>
10. Radogna, Dicato, & Diederich. (2015). Cancer-type-specific crosstalk between autophagy, necroptosis and apoptosis as a pharmacological target. *Biochemical Pharmacology*, 94(1), 1-11.
11. Johnson, D. (2013). *Cell Death Signaling in Cancer Biology and Treatment* (Cell Death in Biology and Diseases).
12. Fadeel, B., & Orrenius, S. (2005). Apoptosis: A basic biological phenomenon with wide-ranging implications in human disease. *Journal of Internal Medicine*, 258(6), 479-517.

13. Gabriel Ichim, & Stephen W. G. Tait. (2016). A fate worse than death: Apoptosis as an oncogenic process. *Nature Reviews Cancer*, 16(8), 539-548.
14. (2011) Necrosis. In: Schwab M. (eds) Encyclopedia of Cancer. Springer, Berlin, Heidelberg
15. Chipuk, Moldoveanu, Llambi, Parsons, & Green. (2010). The BCL-2 Family Reunion. *Molecular Cell*, 37(3), 299-310.
16. Anvekar, R., Asciola, J., Missert, D., & Chipuk, J. (2011). Born to be alive: A role for the BCL-2 family in melanoma tumor cell survival, apoptosis, and treatment. *Frontiers in Oncology*, 1(34), Frontiers in oncology, 13 October 2011, Vol.1(34).
17. Nechushtan, A., Smith, C. L., Hsu, Y. T. and Youle, R. J. (1999). Conformation of the Bax C-terminus regulates subcellular location and cell death *EMBO J.* 18, 2330-2341.
18. Suzuki, M., Youle, R. J. and Tjandra, N. (2000). Structure of Bax: coregulation of dimer formation and intracellular localization. *Cell* 103, 645-654
19. Dewson, G., & Kluck, R. (2009). Mechanisms by which Bak and Bax permeabilise mitochondria during apoptosis. *Journal of Cell Science*, 122(Pt 16), 2801-8.
20. Alex R. D. Delbridge, Stephanie Grabow, Andreas Strasser, & David L. Vaux. (2016). Thirty years of BCL-2: Translating cell death discoveries into novel cancer therapies. *Nature Reviews Cancer*, 16(2), 99-109.
21. Y Suh, I Amelio, T Guerrero Urbano, & M Tavassoli. (2014). Clinical update on cancer: Molecular oncology of head and neck cancer. *Cell Death and Disease*, 5(1), E1018.
22. Sommers, K., Merrick, M.A. Lopez, M.E., Incognito, L.S., Schechter, G.L., & Casey, G. (1992). Frequent p53 Mutations in Head and Neck Cancer: *Cancer Research*, 52: 5997-6000.
23. Loehrer, P. J., Einhorn, L.H. (1984). Cisplatin: *Annals of Internal Medicine*, 100: 704-713.
24. Rosenberg, B., Van Camp, L., Krigas, T. (1965). Inhibition of cell division in *Escherichia coli* by electrolysis products from a platinum electrode. *Nature*. 205: 698-699.
25. Roberts, A.J. (1977). The Mechanism of Action of Anti-tumour Platinum Compounds. *Platinum Metals Rev*, 21(1): 2-15
26. Gutekunst, M., Mueller, T., Weilbacher, A., Dengler, M.A., Bedke, J., Kruck, S., Oren, M., Aulitzky, W.E., van der Kuip, H. (2013). Cisplatin hypersensitivity of testicular germ cell tumors is determined by high constitutive Noxa levels mediated by Oct-4. *Cancer Research*, 73: 1460-1469.

27. Nakajima, W., Sharma, K., Lee, J.Y., Maxim, N.T., Hicks, M.A., Vu, T.T., Luu, A., Yeudall, W.A., Tanake, N., Harada, H. (2016) DNA damaging agent-induced apoptosis is regulated by MCL-1 phosphorylation and degradation mediated by Noxa/MCL-1/CDK2 complex. *Oncotarget*, 7: 36353-36365.
28. Dong Wang, & Stephen J. Lippard. (2005). Cellular processing of platinum anticancer drugs. *Nature Reviews Drug Discovery*, 4(4), 307-320.
29. Ishida, Tomita, Nakashima, Hirata, Tanaka, Shibata, and Hara. "Current Mouse Models of Oral Squamous Cell Carcinoma: Genetic and Chemically Induced Models." *Oral Oncology* 73 (2017): 16-20.
30. Sharma, Kanika, Thien-Trang Vu, Wade Cook, Mitra Naseri, Kevin Zhan, Wataru Nakajima, and Hisashi Harada. "P53-independent Noxa Induction by Cisplatin Is Regulated by ATF3/ATF4 in Head and Neck Squamous Cell Carcinoma Cells." *Molecular Oncology*, 2018, Molecular Oncology, 19 January 2018.
31. Grandis, J., & Tweardy, D. (1993). Elevated levels of transforming growth factor alpha and epidermal growth factor receptor messenger RNA are early markers of carcinogenesis in head and neck cancer. *Cancer Research*, 53(15), 3579-84.
32. Specenier, P., & Vermorken, J. B. (2013). Cetuximab: its unique place in head and neck cancer treatment. *Biologics : Targets & Therapy*, 7, 77-90.
<http://doi.org/10.2147/BTT.S43628>
33. Hijikata M, Kato N, Sato T, Kagami Y, Shimotohno K. (1990). Molecular cloning and characterization of a cDNA for a novel phorbol-12-myristate-13-acetate-responsive gene that is highly expressed in an adult T-cell leukemia cell line. *J Virol* 64: 4632-4639.
34. C Ploner, R Kofler, & A Villunger. (2009). Noxa: At the tip of the balance between life and death. *Oncogene*, 27(S1), S84-S92.
35. Oda E, Ohki R, Murasawa H, Nemoto J, Shibue T, Yamashita T *et al.* (2000). Noxa, a BH3-only member of the Bcl-2 family and candidate mediator of p53-induced apoptosis. *Science* 288: 1053-1058.
36. W Nakajima, M A Hicks, N Tanaka, G W Krystal, & H Harada. (2014). Noxa determines localization and stability of MCL-1 and consequently ABT-737 sensitivity in small cell lung cancer. *Cell Death and Disease*, 5(2), E1052.
37. K M Kozopas, T Yang, H L Buchan, P Zhou, & R W Craig. (1993). MCL1, a gene expressed in programmed myeloid cell differentiation, has sequence similarity to BCL2. *Proceedings of the National Academy of Sciences of the United States of America*, 90(8), 3516-3520.

38. Thomas, L., Lam, C., & Edwards, S. (2010). Mcl-1; the molecular regulation of protein function. *FEBS Letters*, 584(14), 2981-2989.
39. Day, C., Chen, L., Richardson, S., Harrison, P., Huang, D., & Hinds, M. (2005). Solution structure of prosurvival Mcl-1 and characterization of its binding by proapoptotic BH3-only ligands. *The Journal of Biological Chemistry*, 280(6), 4738-44.
40. Chen, Willis, Wei, Smith, Fletcher, Hinds, . . . Huang. (2005). Differential Targeting of Prosurvival Bcl-2 Proteins by Their BH3-Only Ligands Allows Complementary Apoptotic Function. *Molecular Cell*, 17(3), 393-403.
41. J T Opferman. (2006). Unraveling MCL-1 degradation. *Cell Death and Differentiation*, 13(8), 1260-1262.
42. Jorg Michels, Jason W O'Neill, Claire L Dallman, Amalia Mouzakiti, Fay Habens, Matthew Brimmell, . . . Graham Packham. (2004). Mcl-1 is required for Akata6 B-lymphoma cell survival and is converted to a cell death molecule by efficient caspase-mediated cleavage. *Oncogene*, 23(28), 4818-4827.
43. Hail, N., Kim, H., & Lotan, J. (2006). Mechanisms of fenretinide-induced apoptosis. *Apoptosis*, 11(10), 1677-1694.
44. Scher, R., Saito, W., Dodge, R., Richtsmeier, W., & Fine, R. (1998). Fenretinide-Induced Apoptosis of Human Head and Neck Squamous Carcinoma Cell Lines. *Otolaryngology–Head and Neck Surgery*, 118(4), 464-471.
45. Abou-Issa H, Moeschberger M, el-Masry W, Tejwani S, Curley RW Jr, Webb TE (1995) Relative efficacy of glucarate on the initiation and promotion phases of rat mammary carcinogenesis. *Anticancer Res* 15:805–810
46. Ohshima M, Ward JM, Wenk ML (1985). Preventive and enhancing effects of retinoids on the development of naturally occurring skin, prostate gland, and endocrine pancreas in aged male ACI/segHapBR rats. *J Natl Cancer Inst* 74:517–524
47. Chodak GW, Rukstalis D, Kellman HM, Williams M (1993) Phase II study of the retinoid analogue 4-HPR in men with carcinoma of the prostate. *J Urol* 149:25
48. Veronesi U, De Palo G, Marubini E et al (1999) Randomized trial of fenretinide to prevent second breast malignancy in women with early breast cancer. *J Natl Cancer Inst* 91:1847–1856
49. Armstrong, J., Flockhart, R., Veal, G., Lovat, P., & Redfern, C. (2010). Regulation of endoplasmic reticulum stress-induced cell death by ATF4 in neuroectodermal tumor cells. *The Journal of Biological Chemistry*, 285(9), 6091-100.

50. Nabanita Mukherjee, Steven N Reuland, Yan Lu, Yuchun Luo, Karoline Lambert, Mayumi Fujita, . . . Yiquan G Shellman. (2014). Combining a BCL2 Inhibitor with the Retinoid Derivative Fenretinide Targets Melanoma Cells Including Melanoma Initiating Cells. *Journal of Investigative Dermatology*, 135(3), 842-850.
51. Tse, C., Shoemaker, A., Adickes, J., Anderson, M., Chen, J., Jin, S., . . . Elmore, S. (2008). ABT-263: A potent and orally bioavailable Bcl-2 family inhibitor. *Cancer Research*, 68(9), 3421-8.
52. Kaefer, A., Yang, J., Noertersheuser, P., Mensing, S., Humerickhouse, R., Awni, W., & Xiong, H. (2014). Mechanism-based pharmacokinetic/pharmacodynamic meta-analysis of navitoclax (ABT-263) induced thrombocytopenia. *Cancer Chemotherapy and Pharmacology*, 74(3), 593-602.
53. Anthony C. Faber, Anna F. Farago, Carlotta Costa, Anahita Dastur, Maria Gomez-Caraballo, Rebecca Robbins, . . . Jeffrey A. Engelman. (2015). Assessment of ABT-263 activity across a cancer cell line collection leads to a potent combination therapy for small-cell lung cancer. *Proceedings of the National Academy of Sciences*, 112(11), E1288-96.
54. Chessum, N., Jones, K., Pasqua, E., & Tucker, M. (2015). Recent advances in cancer therapeutics. *Progress in Medicinal Chemistry*, 54, 1-63.
55. Michael D Wendt (2008). Discovery of ABT-263, a Bcl-family protein inhibitor: observations on targeting a large protein–protein interaction, Expert Opinion on Drug Discovery, 3:9, 1123-1143, DOI: [10.1517/17460441.3.9.1123](https://doi.org/10.1517/17460441.3.9.1123)
56. Justin Kale, Elizabeth J Osterlund, & David W Andrews. (2017). BCL-2 family proteins: Changing partners in the dance towards death. *Cell Death and Differentiation*, 25(1), 65-80.
57. Zhu, Y., Regunath, K., Jacq, X., & Prives, C. (2013). Cisplatin causes cell death via TAB1 regulation of p53/MDM2/MDMX circuitry. *Genes & Development*, 27(16), 1739-1751.
58. Ewings, K., Wiggins, C., & Cook, S. (2007). Bim and the Pro-Survival Bcl-2 Proteins: Opposites Attract, ERK Repels. *Cell Cycle*, 6(18), 2236-2240.
59. Cardinali, M., Kratochvil, F., Ensley, J., Robbins, K., & Yeudall, W. (1997). Functional characterization in vivo of mutant p53 molecules derived from squamous cell carcinomas of the head and neck. *Molecular Carcinogenesis*, 18(2), 78-88.
60. Bourhis, Lubin, Roche, Koscielny, Bosq, Dubois, . . . Bourhis, J. (1996). Analysis of p53 serum antibodies in patients with head and neck squamous cell carcinoma. *Journal of the National Cancer Institute*, 88(17), 1228-123

61. Hübner, Barrett, Flavell, & Davis. (2008). Multisite Phosphorylation Regulates Bim Stability and Apoptotic Activity. *Molecular Cell*, 30(4), 415-425.

Vita

Erin Lindsey Britt was born on May 3, 1993, in Silver Spring, Maryland, and is an American citizen. She graduated from Our Lady of Good Counsel High School, Olney, Maryland in 2011. Erin received her Bachelor of Science in Biophysics from George Washington University, Washington, District of Columbia in 2016. She then received a Post-Baccalaureate Graduate Certificate from Virginia Commonwealth University, Richmond, Virginia in 2017. Upon completing the certificate program, she joined the Department of Physiology and Biophysics where she began conducting research in Dr. Harada's lab in the summer of 2017, working toward a Master of Science degree. She was accepted into dental school during the following year of her graduate studies and is now chasing her dream of becoming a dentist.